Instrumentation for WIMP Direct Detection

From nuclear recoils to measurable detector signals

Núria Castelló-Mor (IFCA, Santander)

TIDPAN 2026

Historical progress

A Quick Refresher: how to read an upper limit

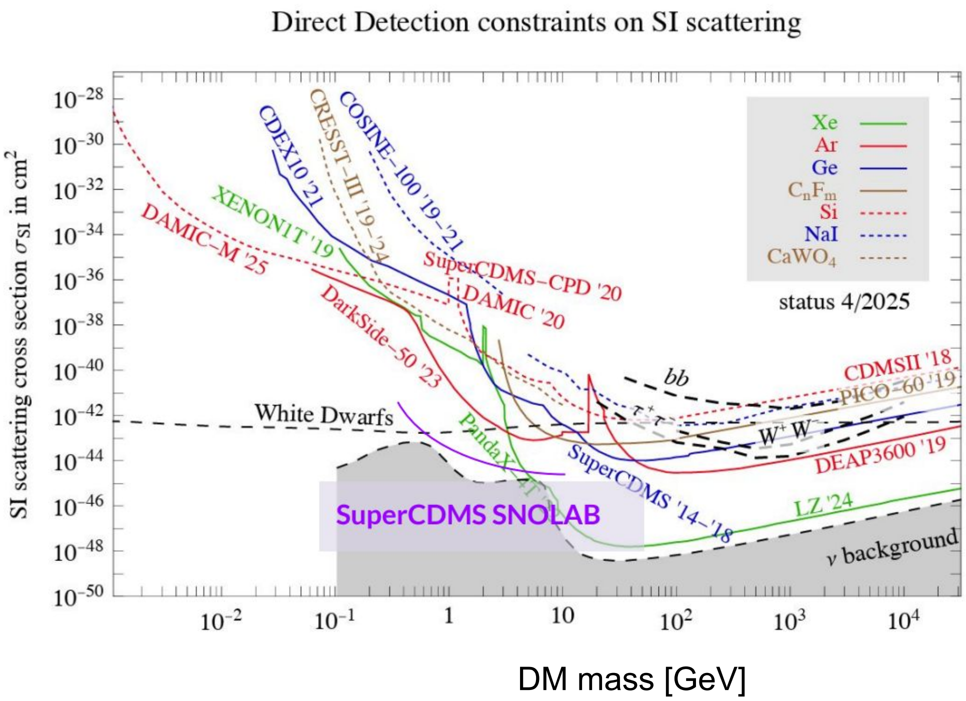

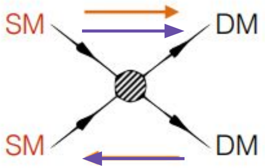

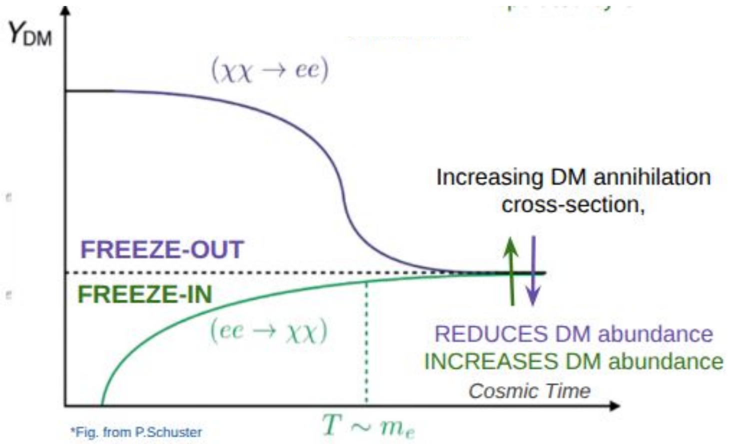

Historical progress

A Quick Refresher: how to read an upper limit

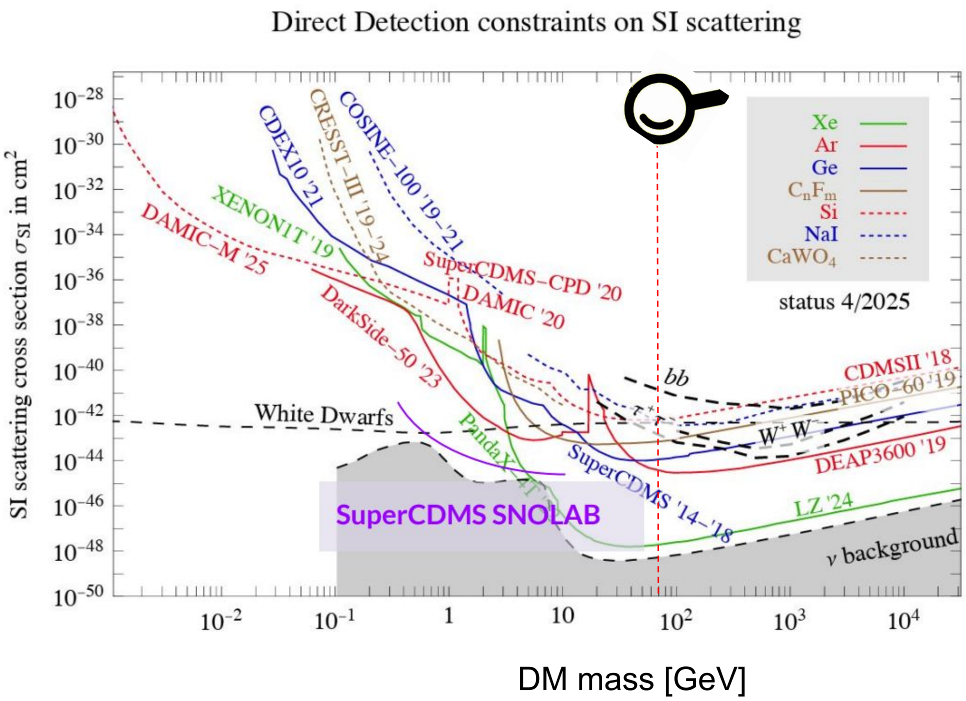

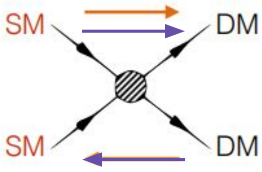

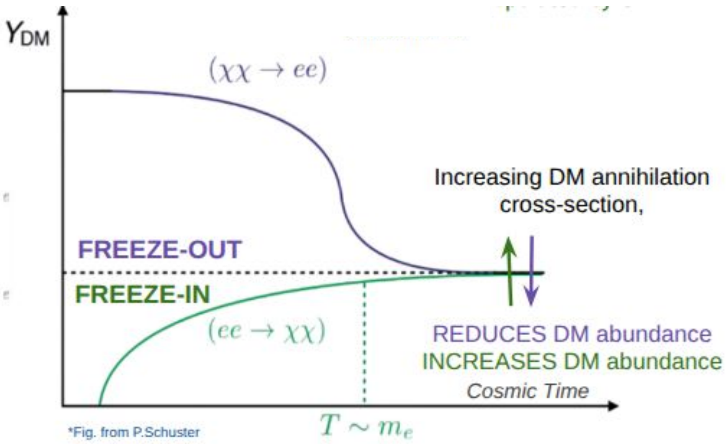

Historical progress

Direct detection has been driven by detector progress

Several orders of magnitude in sensitivity have been gained by improving detector technology, not only by analysis choices alone.

Cleaner materials ⇒ Reduce radioactive backgrounds

Better background rejection ⇒ Distinguish NR / ER

Larger exposures ⇒ Increase the $P_{observing}$ rare events

More stable readout ⇒ Control systematics

Lower thresholds ⇒ smaller E_R accessible

A historical benchmark: SI sensitivity at 60 GeV/c^2

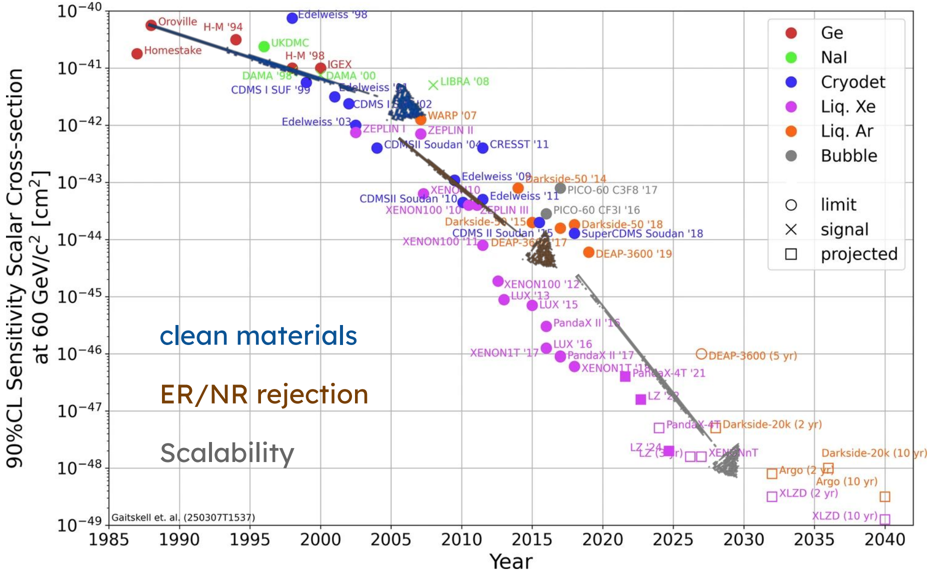

Nature: Commun.Phys. 9 (2026) 1, 105

solid: achieved limits
empty: projected sensitivities

The central detector question

From nuclear recoils to detector observables

How does a **tiny nuclear recoil** become a **measurable detector signal**?

$$\chi + N \to \chi + N$$

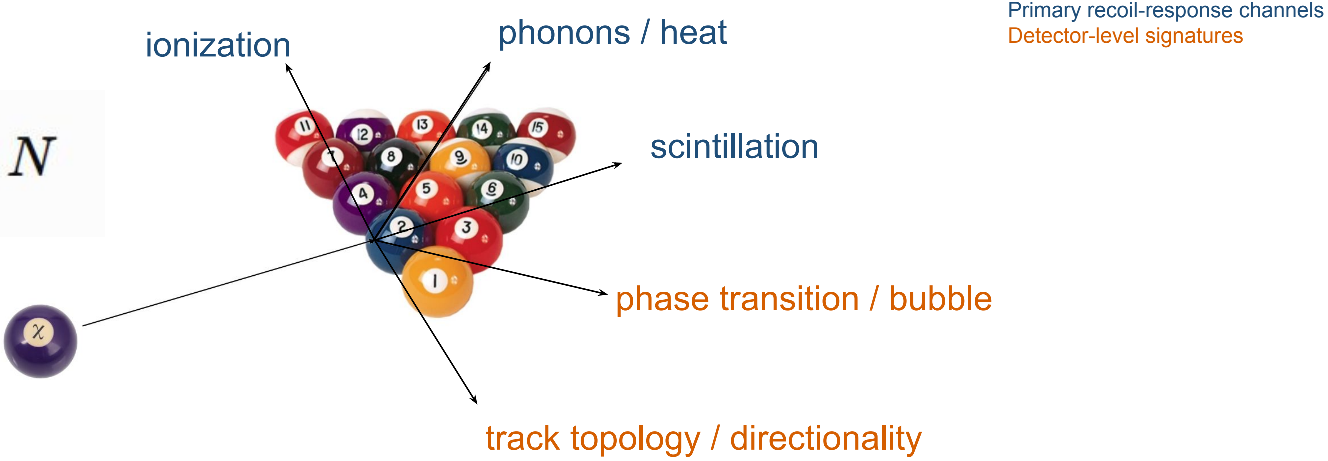

Different detector technologies probe different parts of the recoil response

Scope of this talk

From recoil physics to detector observables

Direct detection is a **chain** of **physical conversions** and **instrumental choices**

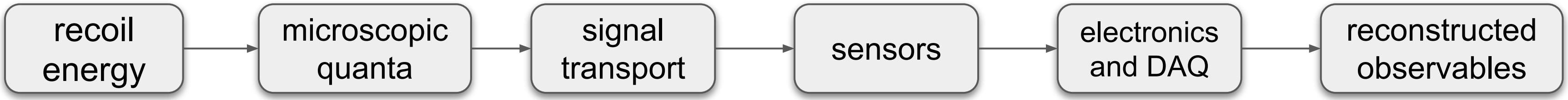

- What microscopic excitations can a recoil generate?
- How do different detectors measure them?
- What instrumental trade-offs define their performance?

The basic WIMP signal

Elastic scattering kinematics: a rare, low-energy nuclear recoil

$$\chi + N \rightarrow \chi + N$$

Elastic recoil kinematics $$E_R = \frac{\mu_{\chi N}^2 v^2}{m_N}(1 - \cos\theta)$$

$$E_R^{\max} = \frac{2\mu_{\chi N}^2 v^2}{m_N}$$

- Galactic WIMPs are non-relativistic: $v \sim 10^{-3}$c
- The standard signal is a single nuclear recoil
- Typical recoil energies are sub-keV to tens of keV
- The recoil spectrum falls steeply with recoil energy

Expected recoil spectrum

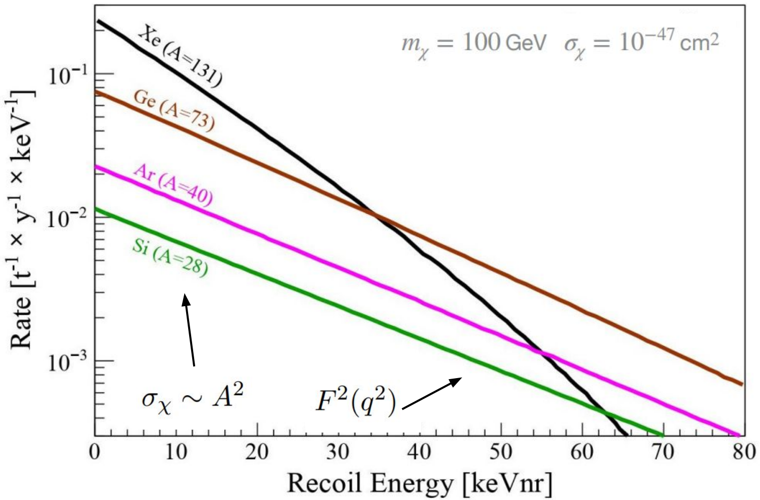

Low thresholds are essential because the WIMP recoil spectrum falls steeply with recoil energy.

Electronic recoils vs nuclear recoils

Nuclear recoils and electronic recoils partition energy differently

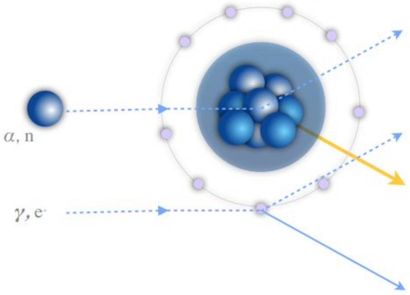

$$Q_{\text{channel}}(E_R) = \frac{\text{visible signal from NR}}{\text{visible signal from ER at same } E_R} < 1$$

NR ionization yield is energy-dependent and below ER yield

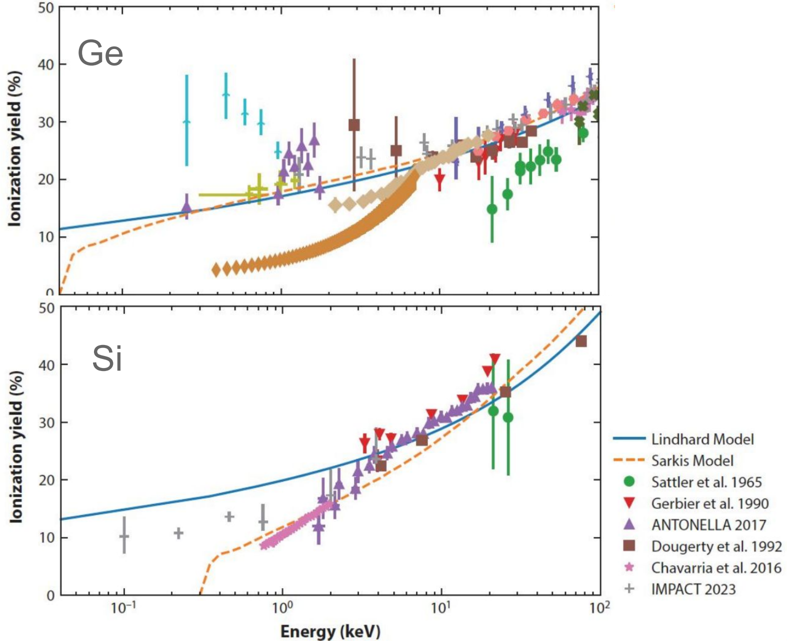

- quenching: reduced visible signal for NR
- ionization yield: charge response
- scintillation efficiency: light response
- ER/NR discrimination: compare signal channels

Channel-specific response parameters:

$$Y_{\text{ion}},\ \mathcal{L}_{eff},\ L_y,\ Q_y,\ \ldots$$

The same recoil energy does not imply the same detector signal

From recoil energy to measurable quanta

Only part of the recoil energy appears in measurable channels

$$E_R = E_{\text{ion}} + E_{\text{scint}} + E_{\text{phonon}} + E_{\text{defects}} + \cdots$$

$E_R \longrightarrow$

- **ionization**
- **scintillation**
- **phonons / heat**
- **defects / invisible channels**

  → energy not directly measured

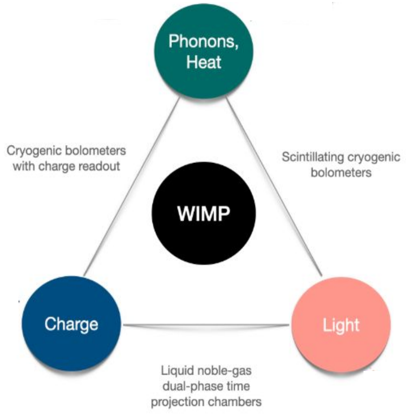

Detector threshold is set by measurable quanta, not by recoil energy alone.

Main signal channels in WIMP detectors

We will now **look** at the **anatomy of a detector signal** in **representative technologies**.

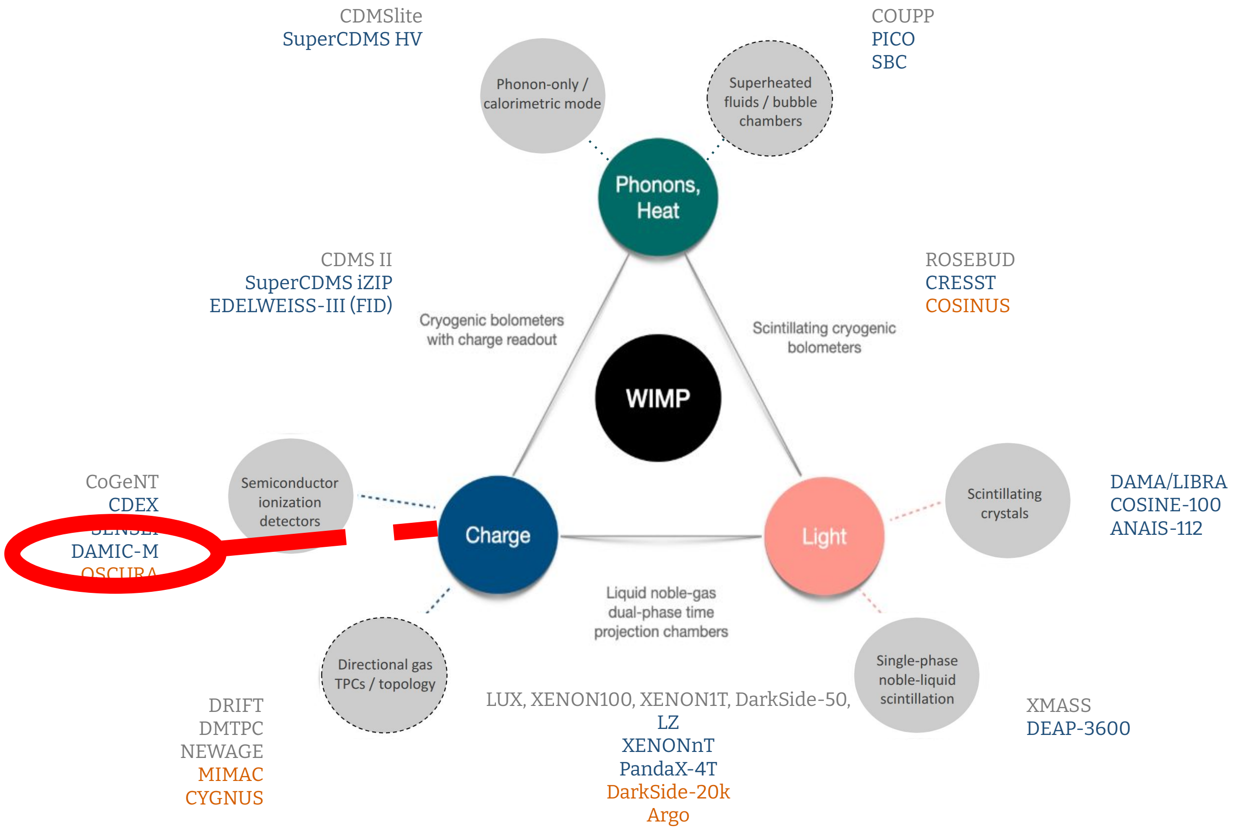

historical / precursor / completed
current / flagship
future / planned / emerging

→ The vertices represent the main microscopic signal channels: charge, light, and phonons or heat.
→ The edges correspond to technologies that combine two signal channels.
→ The dashed external circles represent detector-level signatures not described by one microscopic channel alone.

Charge readout: silicon skipper CCDs

Representative experiments: SENSEI, DAMIC-M, OSCURA

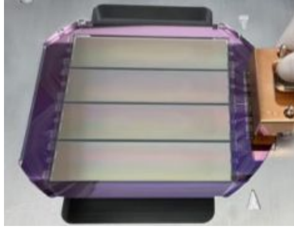

Signal Anatomy

$E_R \rightarrow e^{-}h^{+}$ pairs $\rightarrow$ drift in depleted Si

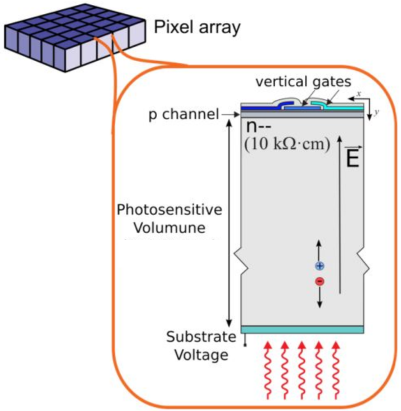

15 μm x 15 μm x 670 μm

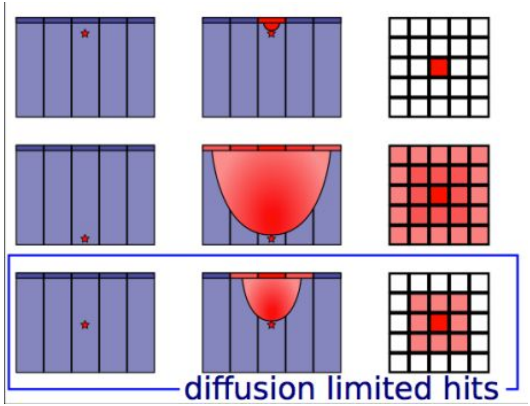

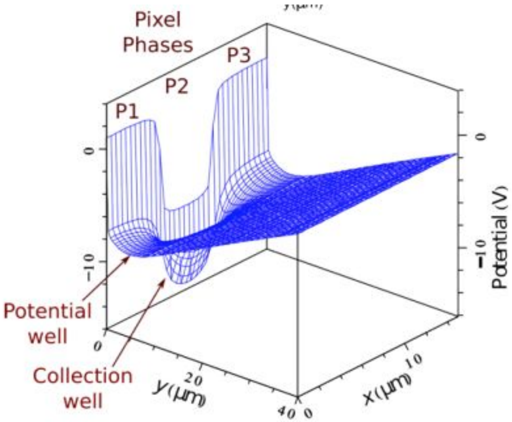

Charge readout: silicon skipper CCDs

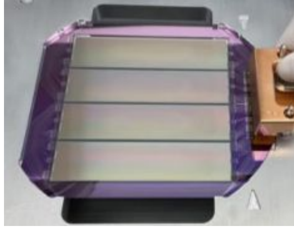

Representative experiments: SENSEI, DAMIC-M, OSCURA

Signal Anatomy

E_R → e^-h^+ pairs → drift in depleted Si → pixel collection

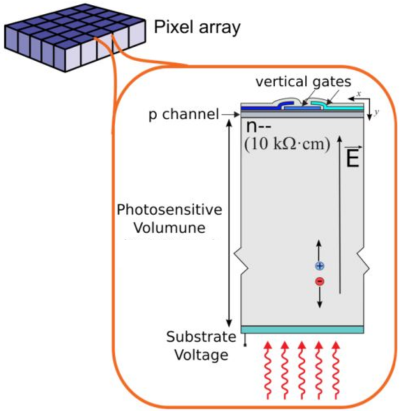

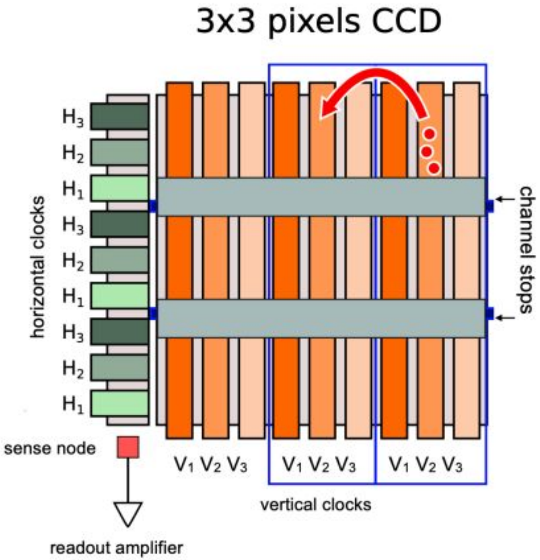

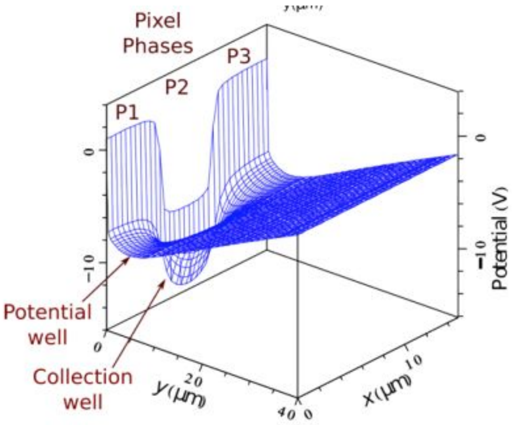

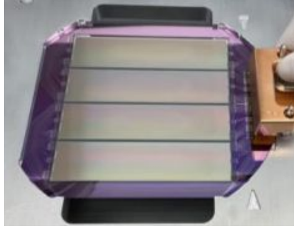

Charge readout: silicon skipper CCDs

Representative experiments: SENSEI, DAMIC-M, OSCURA

Signal Anatomy

$E_R \rightarrow e^- h^+$ pairs $\rightarrow$ drift in depleted Si $\rightarrow$ pixel collection $\rightarrow$ skipper readout $\rightarrow n_e$

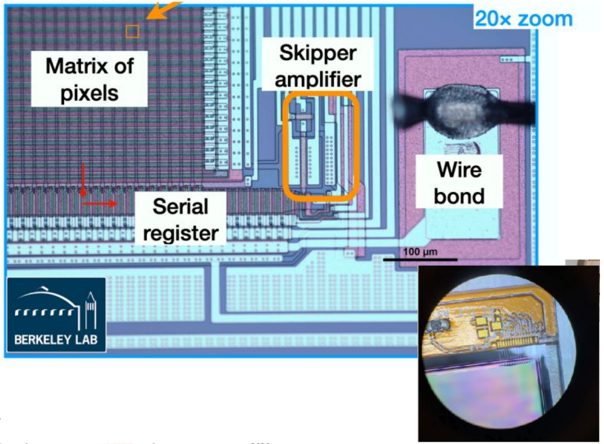

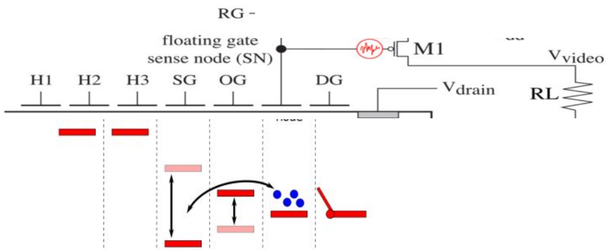

Noise vs number of skips per pixel

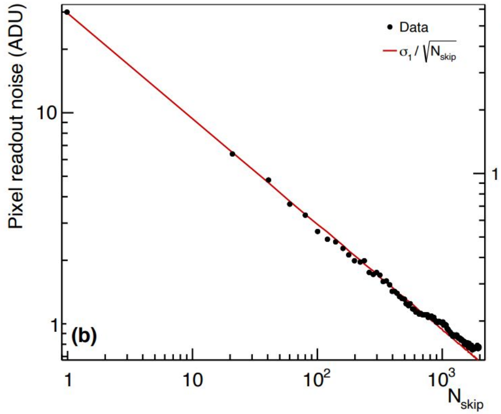

single gaussian peaks → n_e

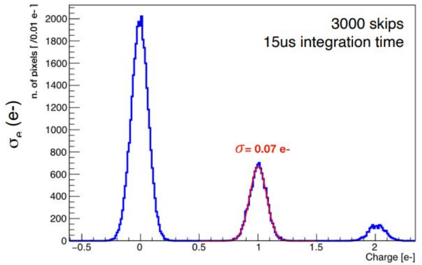

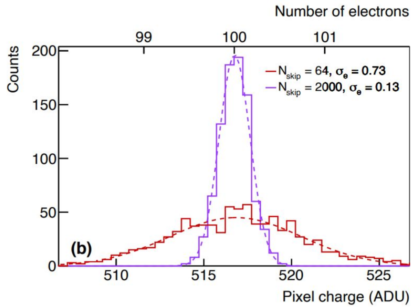

Charge readout: silicon skipper CCDs

Representative experiments: SENSEI, DAMIC-M, OSCURA

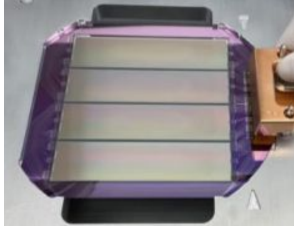

Signal Anatomy

$E_R \rightarrow e^-h^+$ pairs → drift in depleted Si → pixel collection → skipper readout → n_e

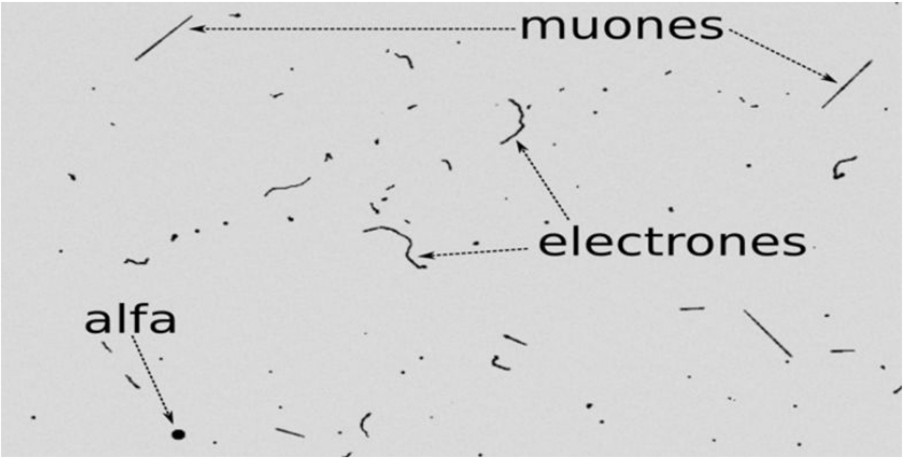

3D reconstruction: particle ID

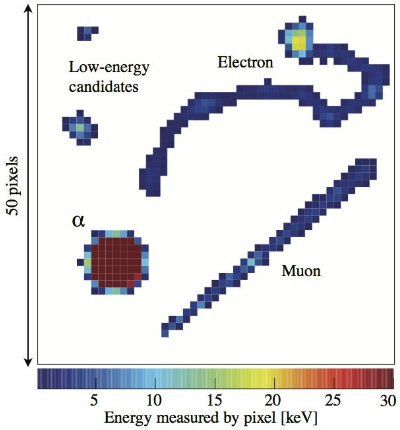

Pros: single-electron resolution, eV-scale threshold, fine spatial granularity, low dark-current rates

Cons: limited target mass, no precise timing, slow readout, limited event-by-event NR/ER discrimination

Charge readout: The DAMIC-M Experiment

DArk **M**atter w**I**th **C**CDs at **M**odane

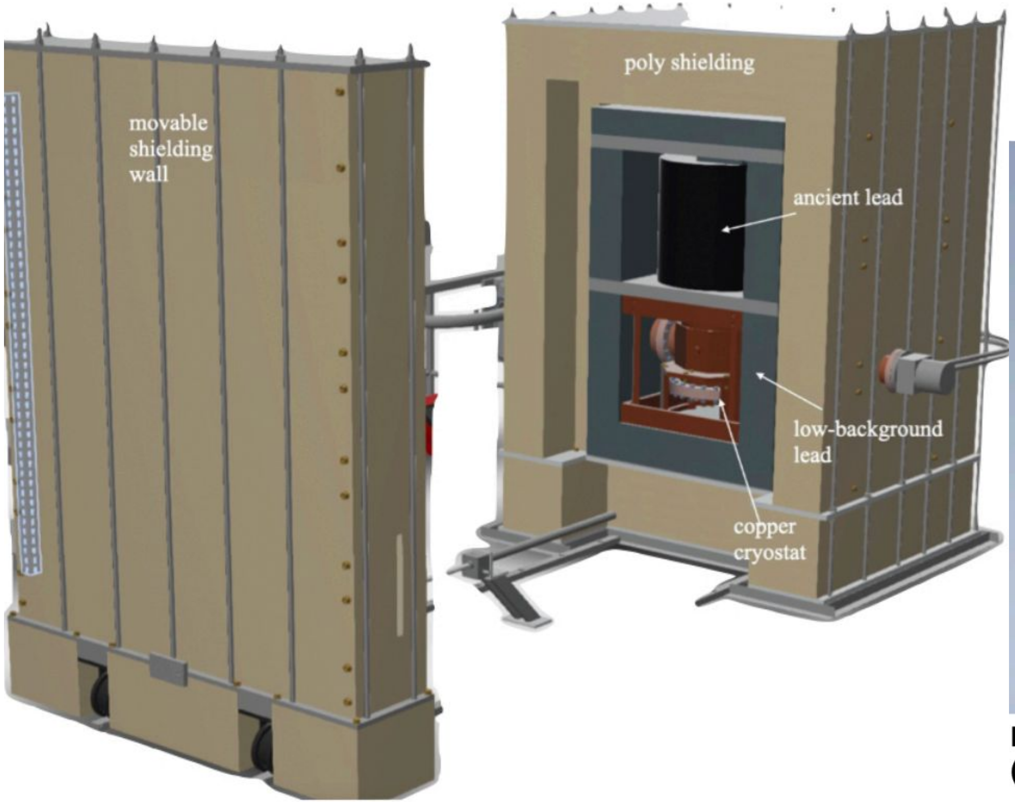

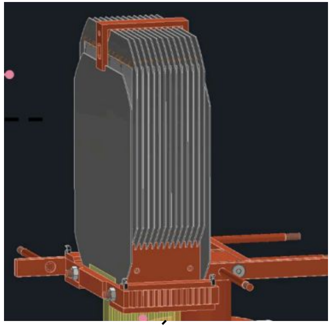

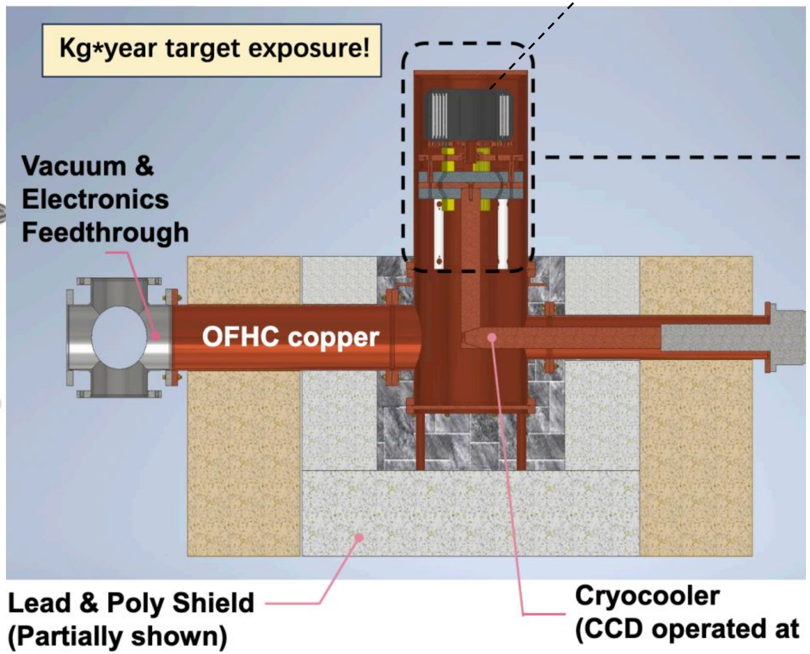

Main signal channels in WIMP detectors

We will now **look** at the **anatomy of a detector signal** in **representative technologies**.

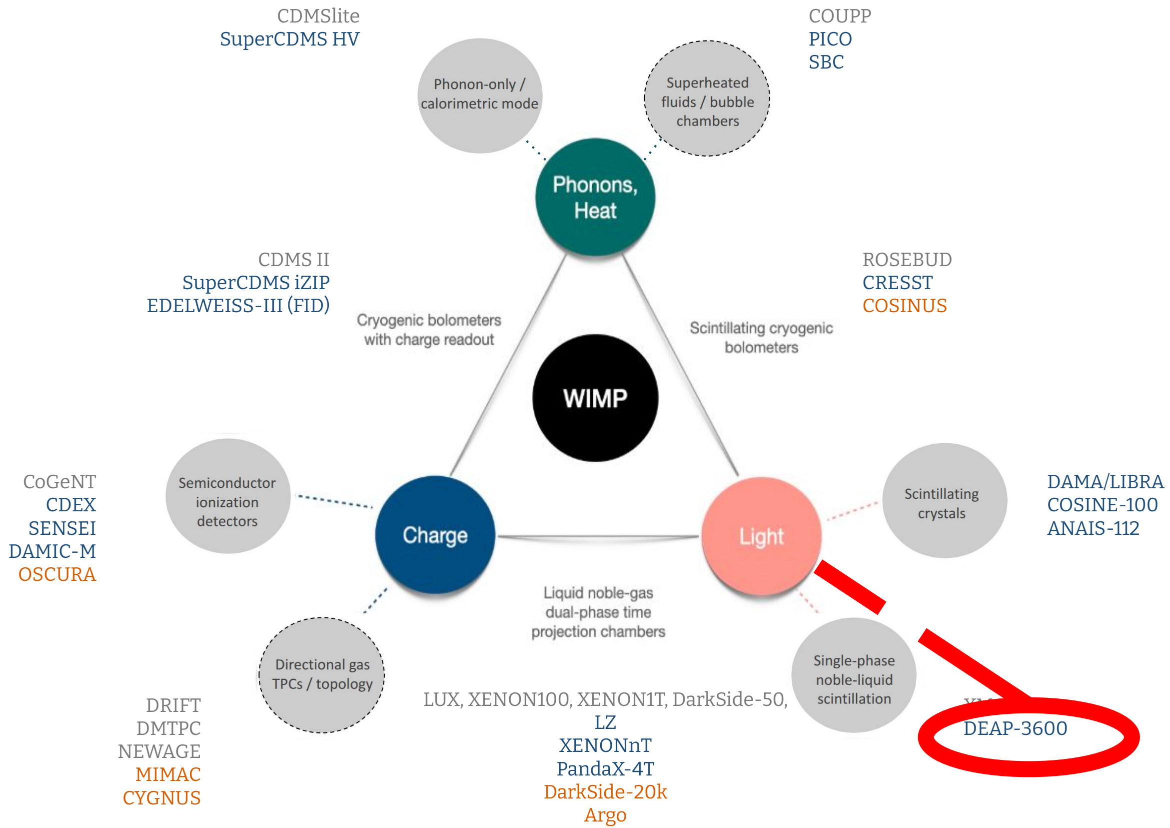

historical / precursor / completed
current / flagship
future / planned / emerging

→ The vertices represent the main microscopic signal channels: charge, light, and phonons or heat.
→ The edges correspond to technologies that combine two signal channels.
→ The dashed external circles represent detector-level signatures not described by one microscopic channel alone.

Light readout: single-phase LAr scintillator

Representative experiments: DEAP-3600

Signal Anatomy

$E_R \rightarrow Ar^*/Ar^+ \rightarrow Ar_2^* \rightarrow$ VUV photons → TPB (wavelength shifting) → visible photons → PMTs

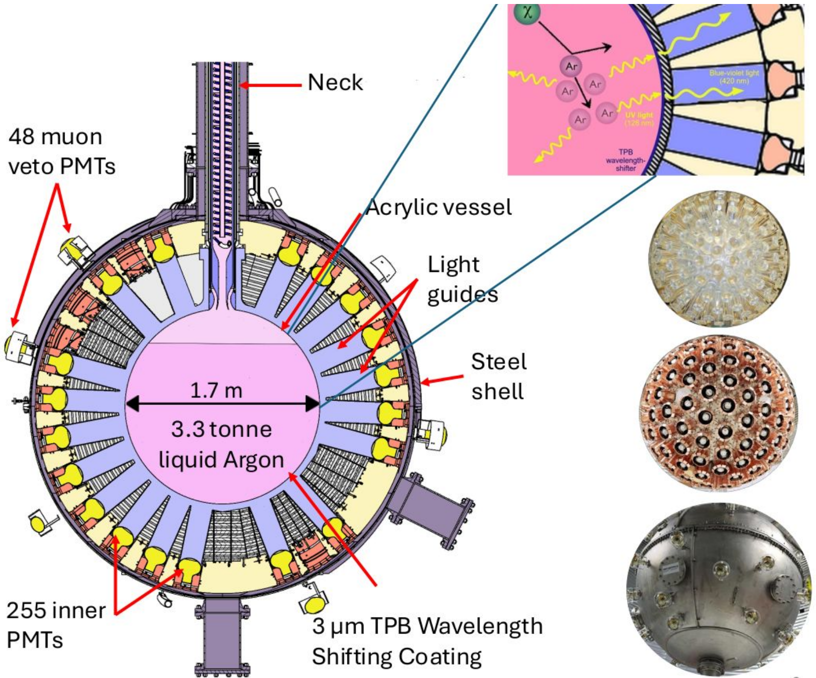

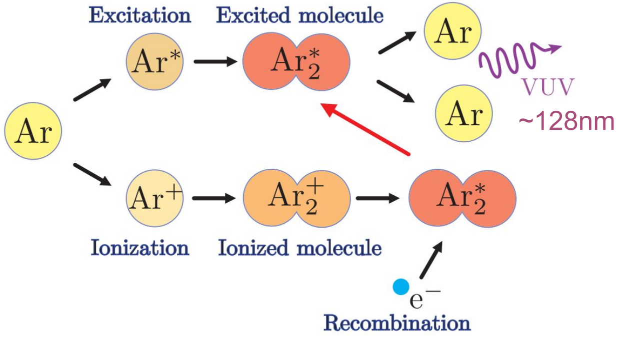

TPB: tetraphenyl butadine (128nm → ~420 nm)
PMTs: photomultiplier tubes

Light readout: single-phase LAr scintillator

Representative experiments: DEAP-3600

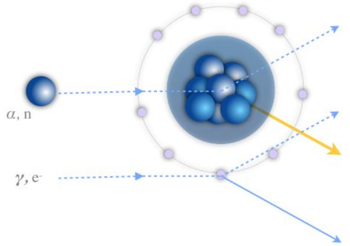

Signal Anatomy

$E_R \rightarrow Ar^*/Ar^+ \rightarrow Ar_2^* \rightarrow$ VUV photons → TPB (wavelength shifting) → visible photons → PMTs → S(t) → $N_{PE}(t)$

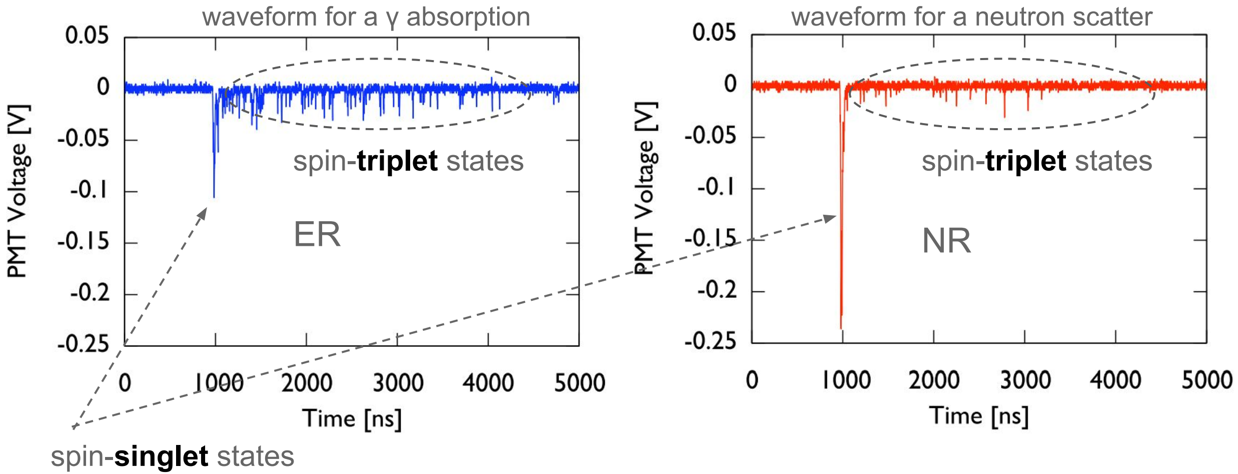

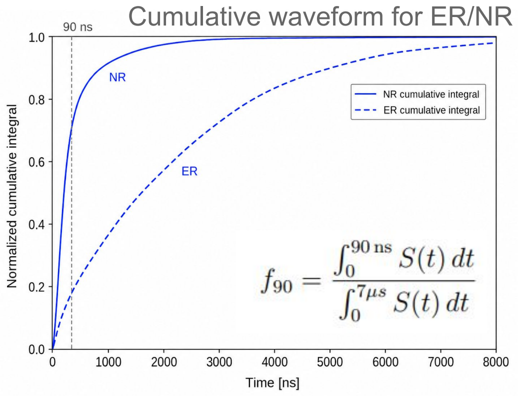

$$\tau_s \simeq 6 \text{ ns}, \qquad \tau_t \simeq 1.3 - 1.6\ \mu\text{s}$$

$$\tau_s \lesssim \Delta t_{\mathrm{DAQ}} \ll \tau_t$$

ER → lower ionization density → larger triplet component → slower pulse (f_{90}~0.3)

NR → higher ionization density → larger singlet component → more prompt pulse (f_{90}~0.7)

Light readout: single-phase LAr scintillator

Representative experiment: DEAP-3600

Signal Anatomy

$E_R \rightarrow Ar^*/Ar^+ \rightarrow Ar_2^* \rightarrow$ VUV photons $\rightarrow$ TPB (wavelength shifting) $\rightarrow$ visible photons $\rightarrow$ PMTs $\rightarrow S(t) \rightarrow N_{PE}(t)$

How much of the light arrived promptly?

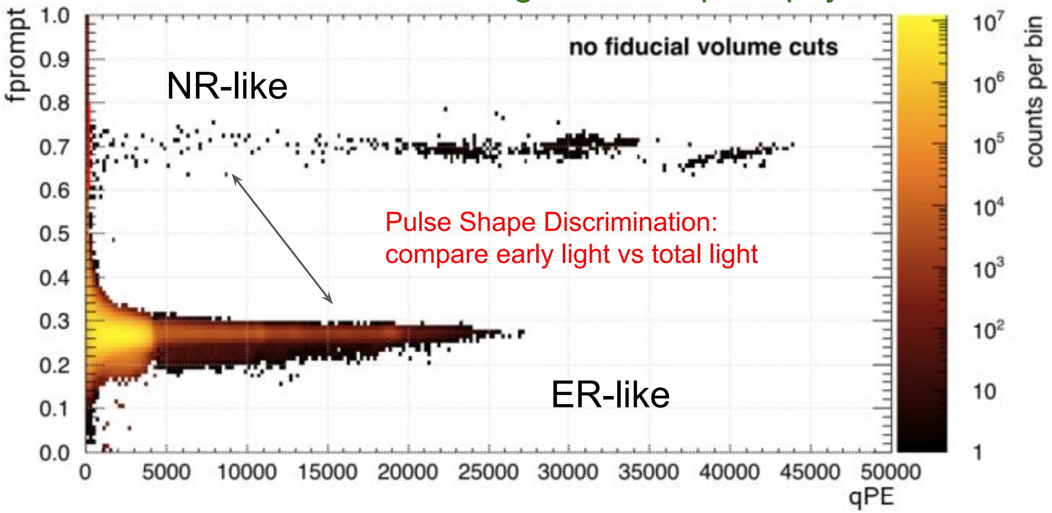

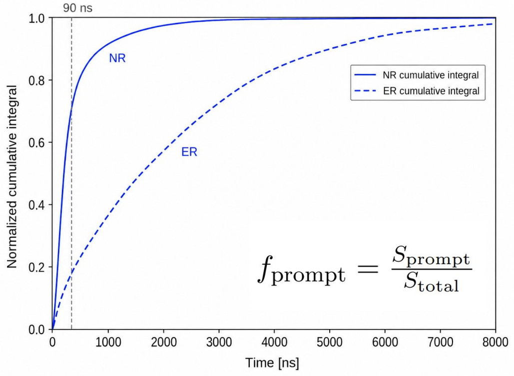

LAr: $\tau_{singlet} \approx 7$ ns ; $\tau_{triplet} \approx 1600$ ns $\Rightarrow$ PSD

LXe: : $\tau_{singlet} \approx 4$ ns ; $\tau_{triplet} \approx 22$ ns $\Rightarrow$ NO PSD

Light readout: single-phase LAr vs Na(Tl) scintillator crystals

DEAP-3600:

E_R → Ar^*/Ar^+ → Ar_2^* → VUV photons → TPB (wavelength shifting) → visible photons → PMTs → S(t) → N_{PE}(t) → PSD

ANAIS-112:

E_R → NaI(Tl) lattice excitations / ionization → Tl activator centers → visible photons → PMTs → S(t) → qPE → Eee → R(E,t)

Strategy: ultra-low background, large exposure, long-term stability, annual modulation in the low-energy rate

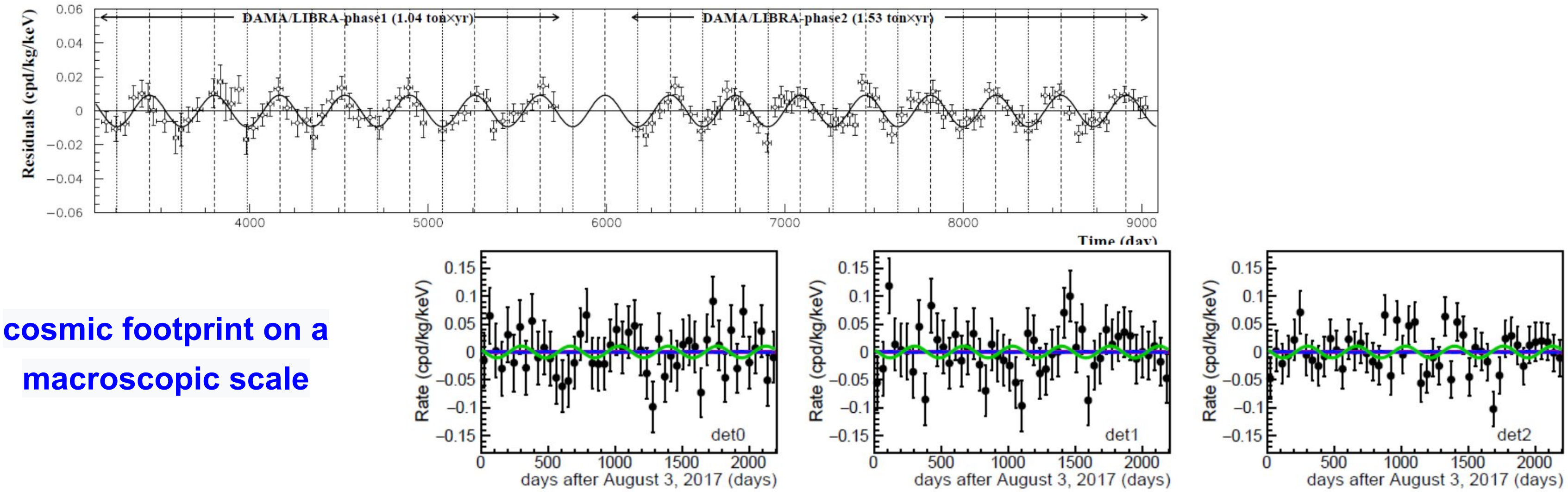

cosmic footprint on a macroscopic scale

Main signal channels in WIMP detectors

We will now **look** at the **anatomy of a detector signal** in **representative technologies**.

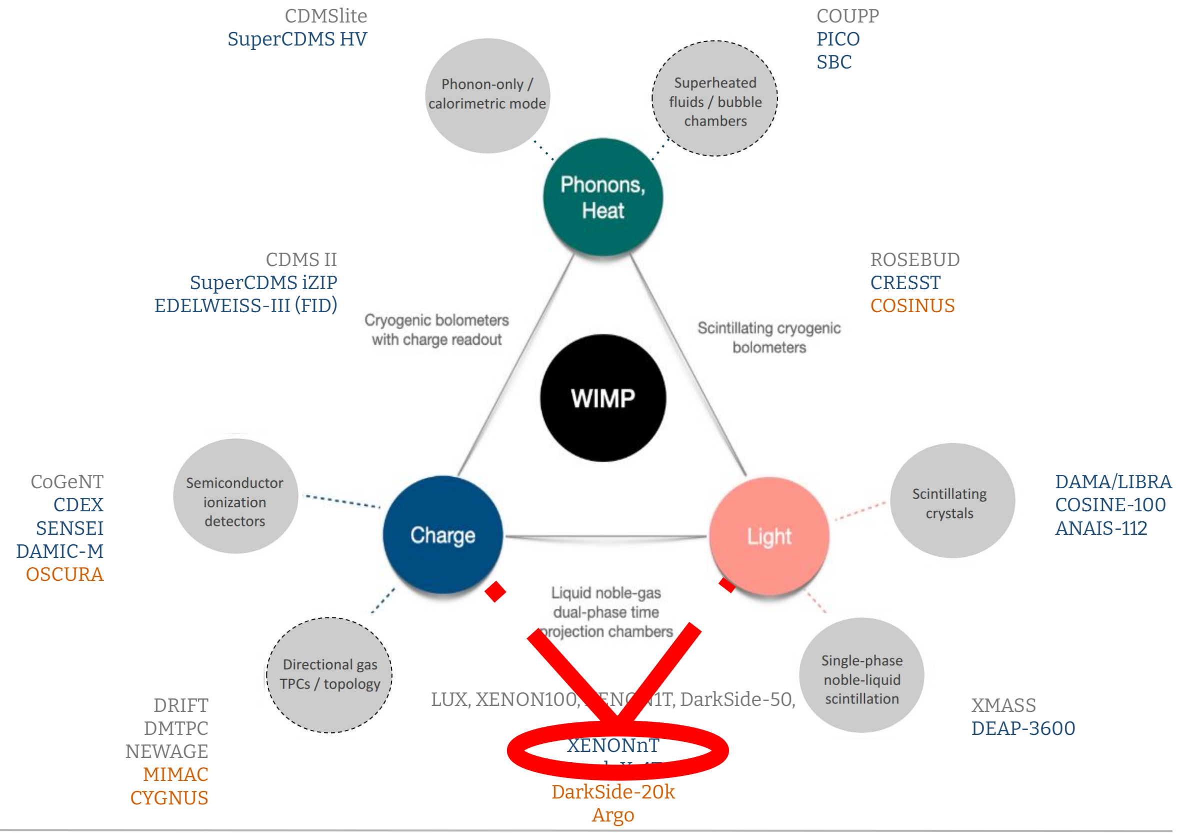

historical / precursor / completed
current / flagship
future / planned / emerging

→ The vertices represent the main microscopic signal channels: charge, light, and phonons or heat.
→ The edges correspond to technologies that combine two signal channels.
→ The dashed external circles represent detector-level signatures not described by one microscopic channel alone.

Charge + Light readout: Dual-phase noble-liquid TPCs

Representative experiments: XENONnT, LZ, PandaX-4T, [LAr: DarkSide-50, DarkSide-20k]

Signal Anatomy

$E_R \rightarrow Xe^{*}/Xe^{+} \rightarrow Xe_2^{*} \rightarrow$ S1 scintillation + e^- drift → extraction to gas → S2 electroluminescence → PMTs → (S1,S2,x,y,z)

253PMTs

241PMTs

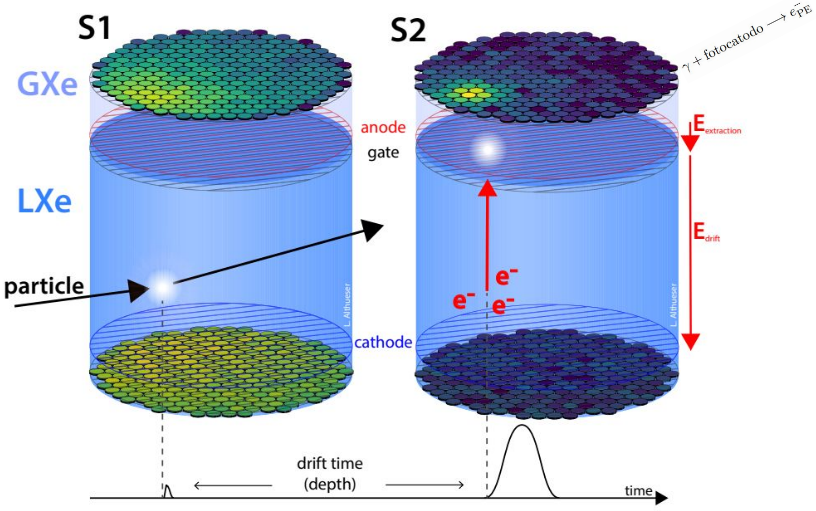

Dual-phase TPCs convert one interaction into two light signals

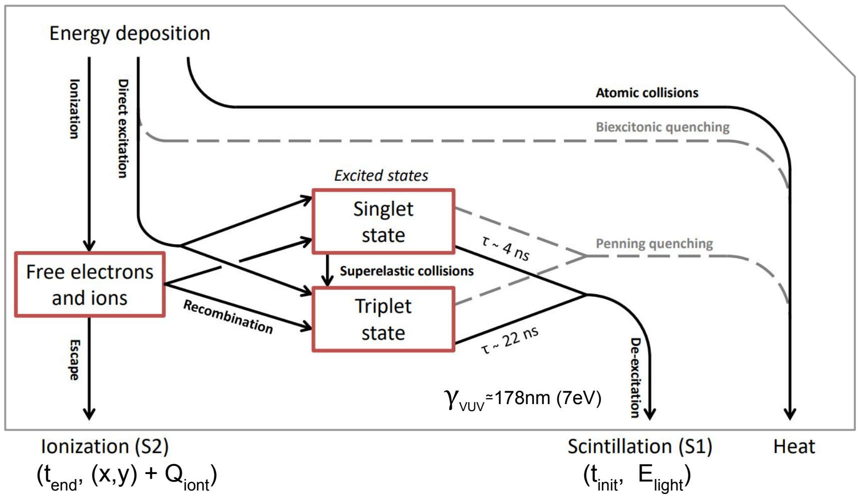

Angevaare, J. R. (2023)

$$\tau_s^{\mathrm{Xe}}, \tau_t^{\mathrm{Xe}} \sim \mathcal{O}(1-10\ \mathrm{ns}) \sim \Delta t_{\mathrm{DAQ}} \sim \sigma_{\mathrm{TTS_{PMT}}} \Rightarrow \text{NO PSC}$$

*Time Projection Chamber (TPC)

Charge + Light readout: Dual-phase noble-liquid TPCs

Representative experiments: XENONnT, LZ, PandaX-4T, [LAr: DarkSide-50, DarkSide-20k]

Signal Anatomy

$E_R \rightarrow Xe^*/Xe^+ \rightarrow Xe_2^* \rightarrow$ S1 scintillation + e^- drift → extraction to gas → S2 electroluminescence → PMTs → (S1,S2,x,y,z)

S1-S2 identified par during a ^{241}AmBe calibration run (NR due to its position on the S2/S1 diagram)

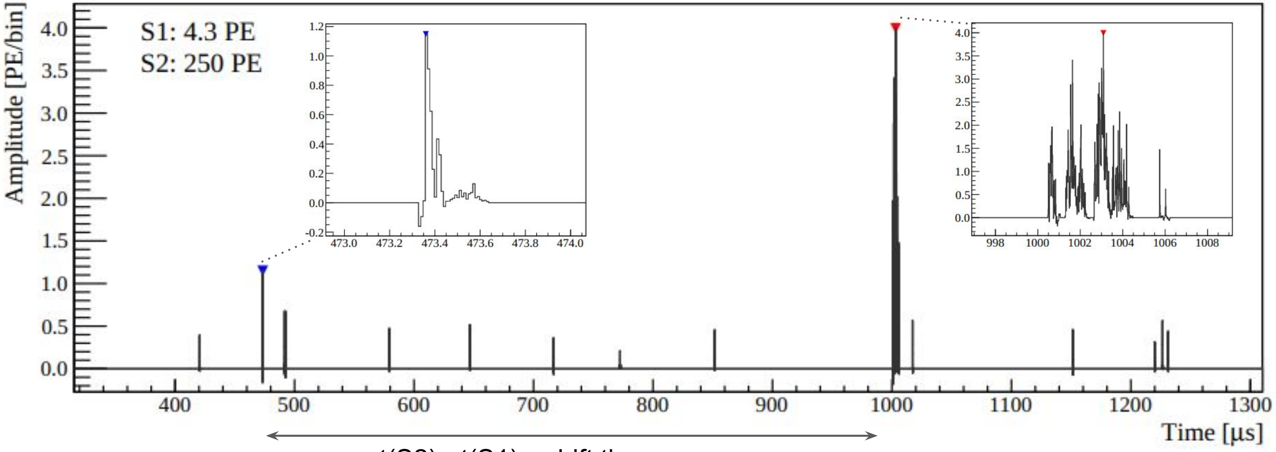

t(S2) - t(S1) = drift time

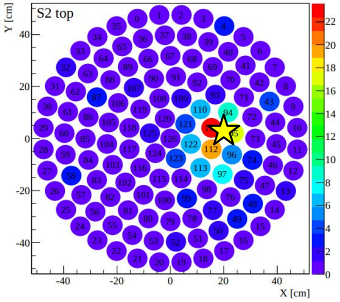

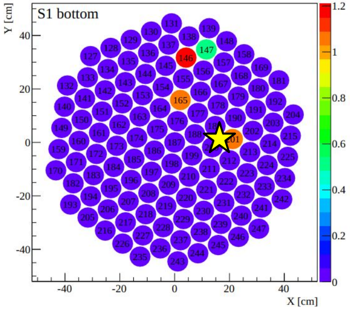

*low-A not correlated

Charge + Light readout: Dual-phase noble-liquid TPCs

Representative experiments: XENONnT, LZ, PandaX-4T, [LAr: DarkSide-50, DarkSide-20k]

Signal Anatomy

$E_R \rightarrow Xe^*/Xe^+ \rightarrow Xe_2^* \rightarrow$ S1 scintillation + e^- drift $\rightarrow$ extraction to gas $\rightarrow$ S2 electroluminescence $\rightarrow$ PMTs $\rightarrow$ (S1,S2,x,y,z)

ER/NR discrimination based on the charge-to-light ratio

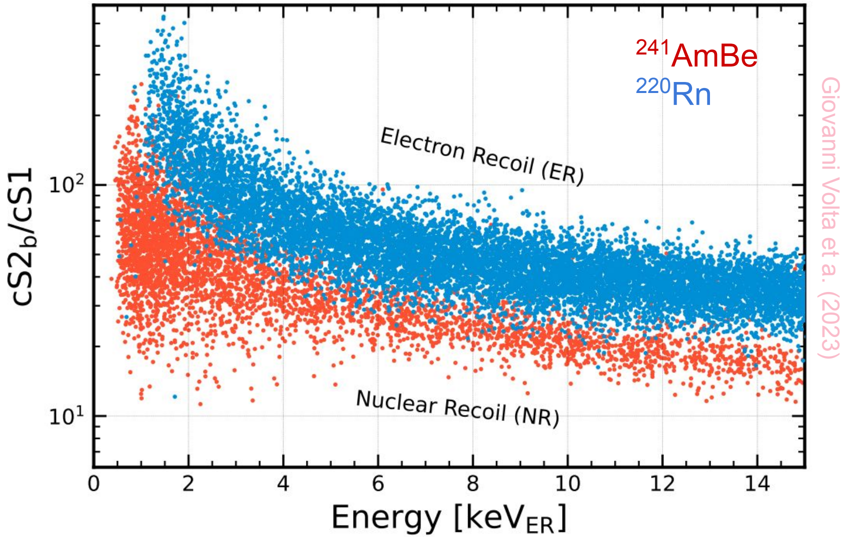

[b]Only-bottom PMT array
[c]corrected from detector response

Dual-phase LXe TPC: The XENON1T Experiment

arXiv:2112.05629

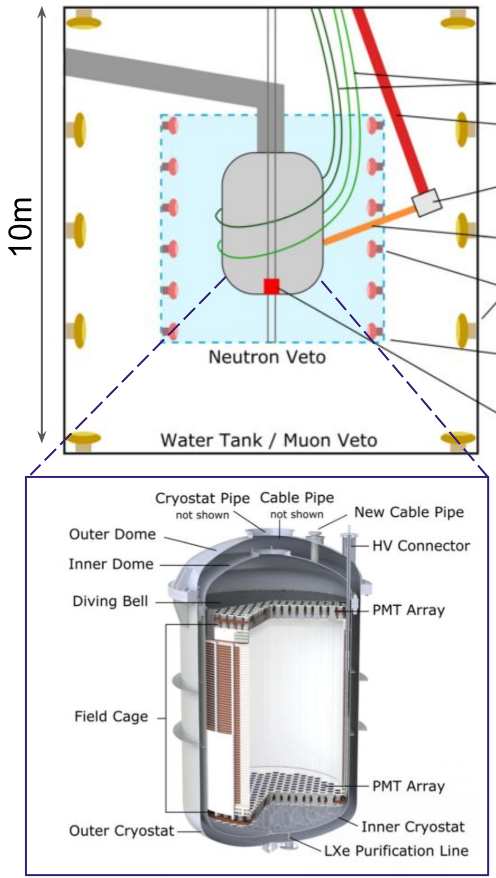

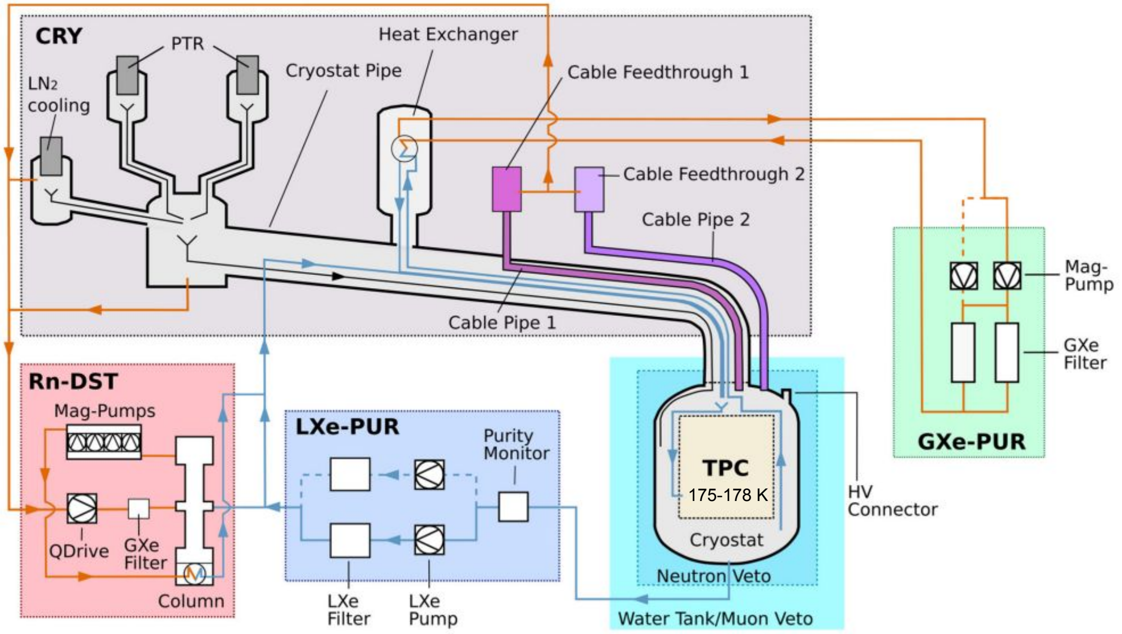

CRY: keeps LXe stable at ~175–178 K

GXe/LXe-Pur: removes electronegative impurities(O_2, H_2O) → preserves S2

Rn-DST: removes radon → reduces internal ER backgrounds

Water + neutron veto: shields and tags muon/neutrons

Main signal channels in WIMP detectors

We will now **look** at the **anatomy of a detector signal** in **representative technologies**.

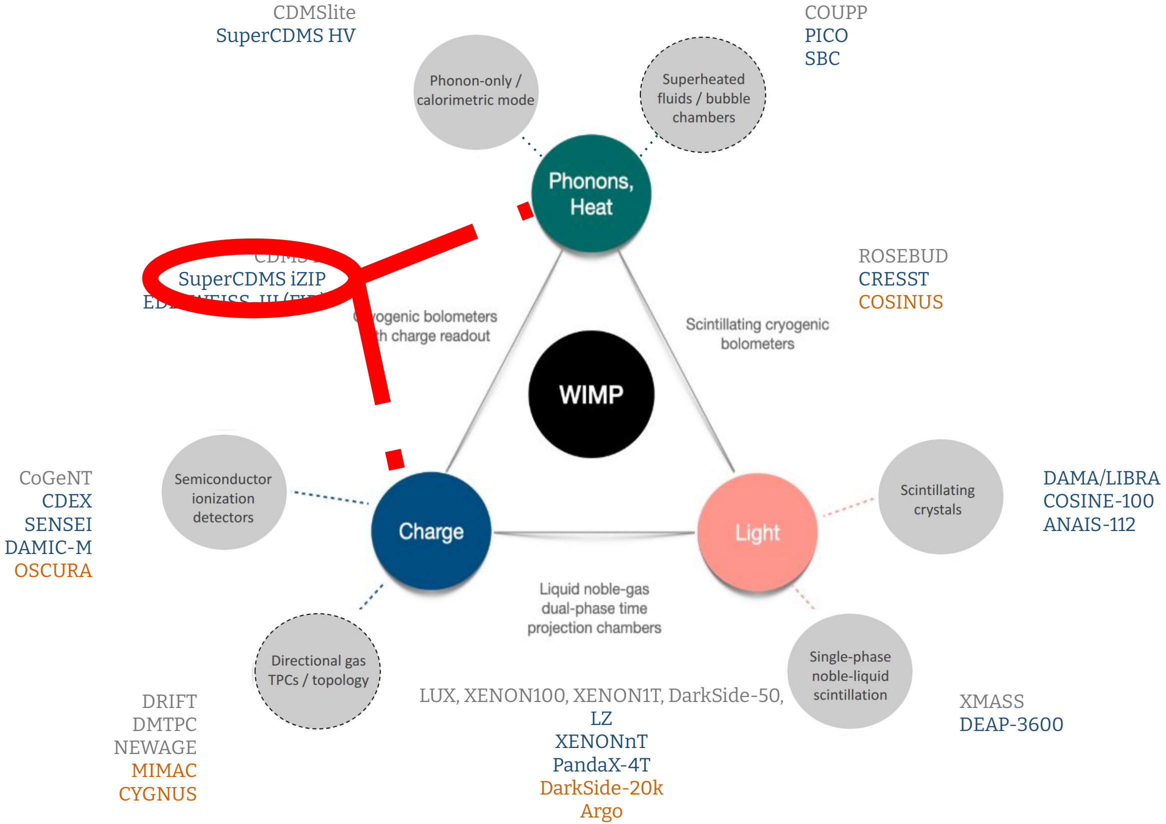

historical / precursor / completed
current / flagship
future / planned / emerging

→ The vertices represent the main microscopic signal channels: charge, light, and phonons or heat.
→ The edges correspond to technologies that combine two signal channels.
→ The dashed external circles represent detector-level signatures not described by one microscopic channel alone.

Charge and phonons: cryogenic semiconductor

Representative experiments: SuperCDMS HV

Athermal phonon sensors

- Energy deposition in detector crystal creates charges and prompt phonons.
- Drifting charges create additional phonons via NTL (Neganov-Trofimov-Luke) effect.
- Phonons are measured by QETs (Quasiparticle trap assisted Electrothermal feedback Transition edge sensors).

$E_{phonon} > 2\Delta$~meV

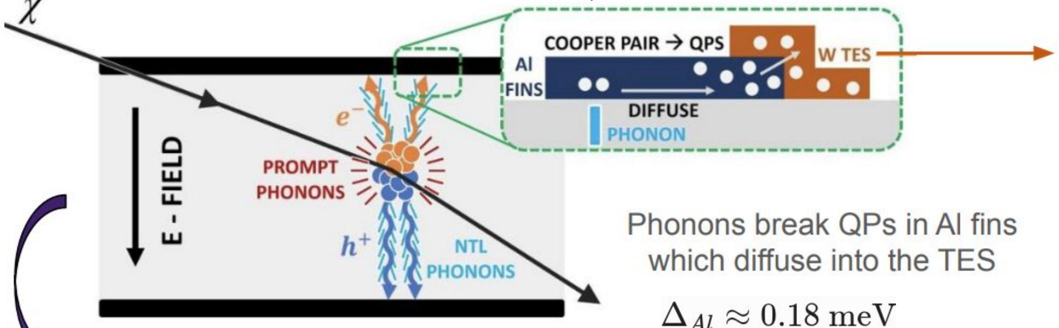

Voltages biases usually O(10-100 V)

Phonons break QPs in Al fins which diffuse into the TES

$$\Delta_{Al} \approx 0.18 \text{ meV}$$

$$\Delta_{W} \approx 0.015 \text{ meV}$$

Measuring phonons with QTEs

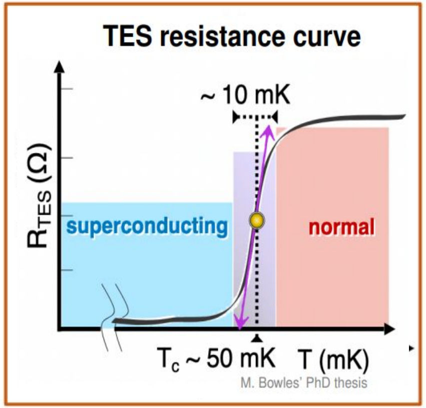

A recoil in a **cold Si/Ge crystal produces prompt phonons** and **charge carriers**. At mK temperatures, the heat capacity is very small, so **a tiny deposited energy can produce a measurable phonon signal**.

Charge and phonons: cryogenic semiconductor

Representative experiments: SuperCDMS HV

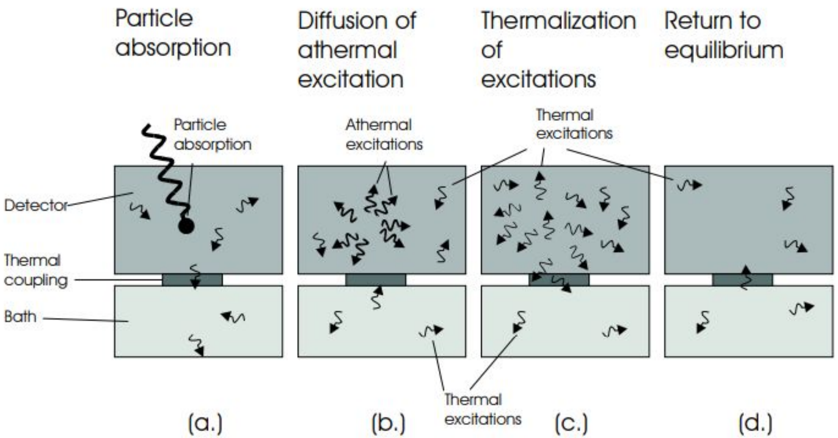

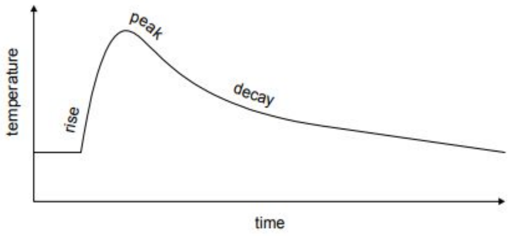

$$Q_{\text{channel}}(E_R) = \frac{\text{visible signal from NR}}{\text{visible signal from ER at same } E_R} < 1$$

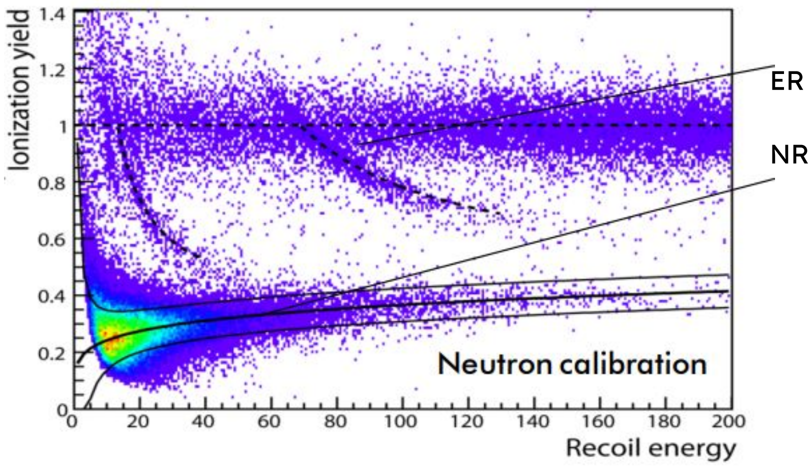

Charge and phonons: cryogenic semiconductor

Signal Anatomy

E_R → e-h pairs + prompt phonons → e-h drift in HV →additional NTL phonon → QET/TES phonon readout → E_{phonon} and Y_{ion}

iZIP (interleaved Z-sensitive Ionization and Phonon) detectors

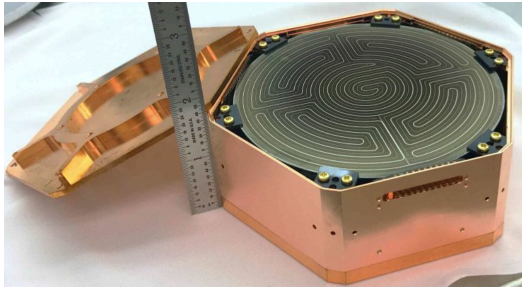

- Measure charge and phonons (Y_{ion})
- Discrimination between NR and ER

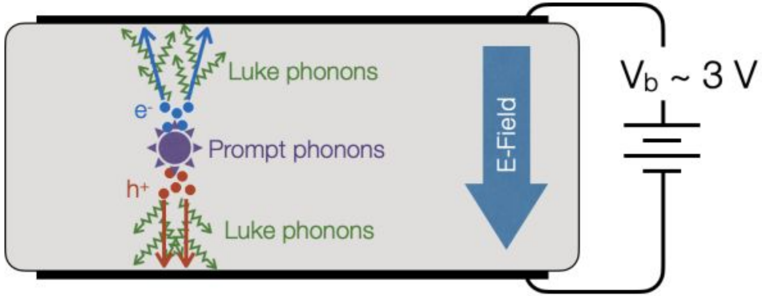

HV (High Voltage) detectors

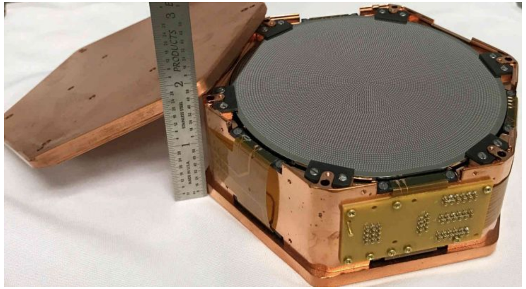

- Amplified NTL phonon production
- Better energy resolution and lower threshold

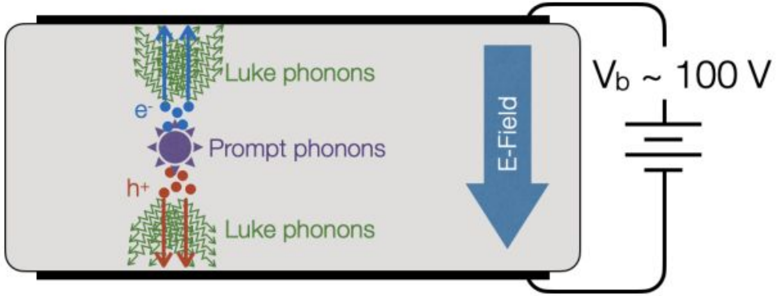

Charge + Phonon readout: iZIP

$$E_t = E_R \left[1 + \frac{Y_{ion}(E_R) V_b}{\epsilon} \right]$$

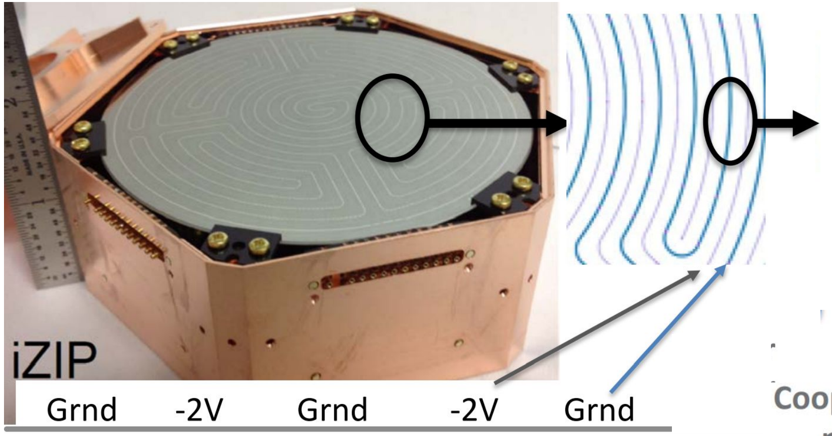

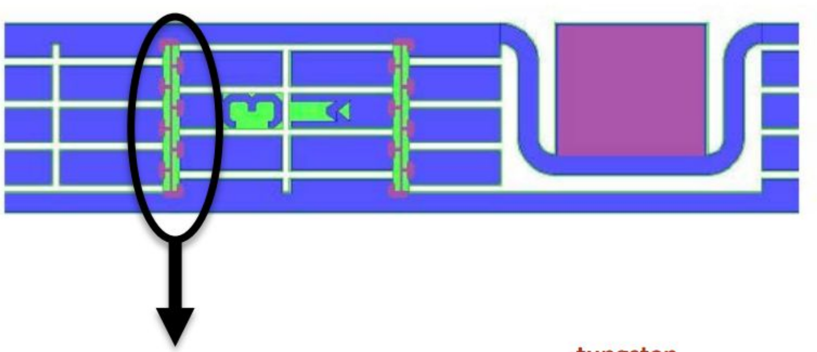

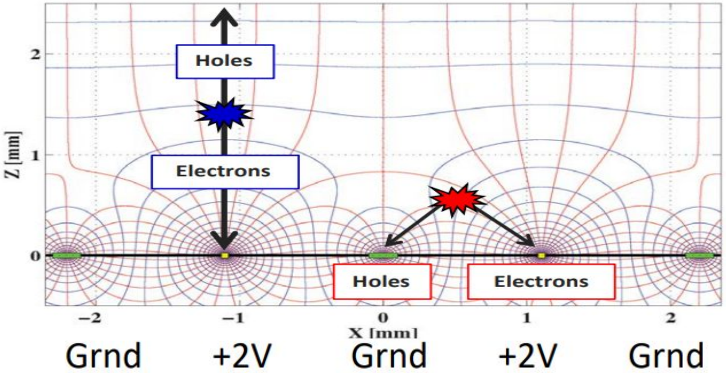

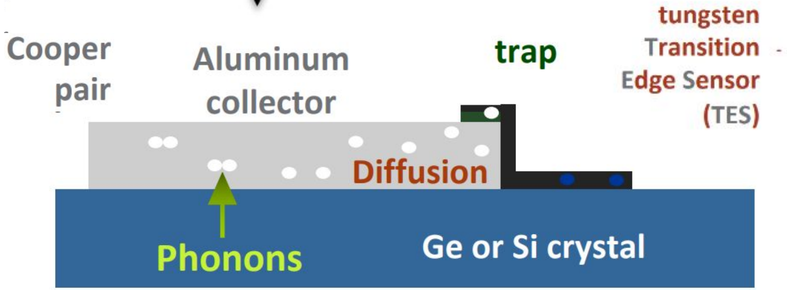

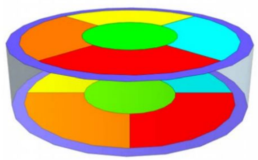

Phonon readout: HV

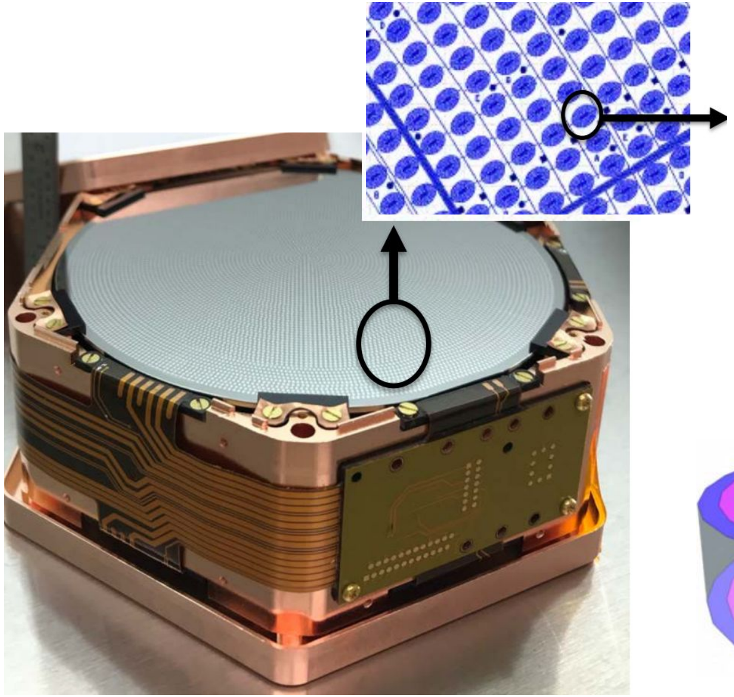

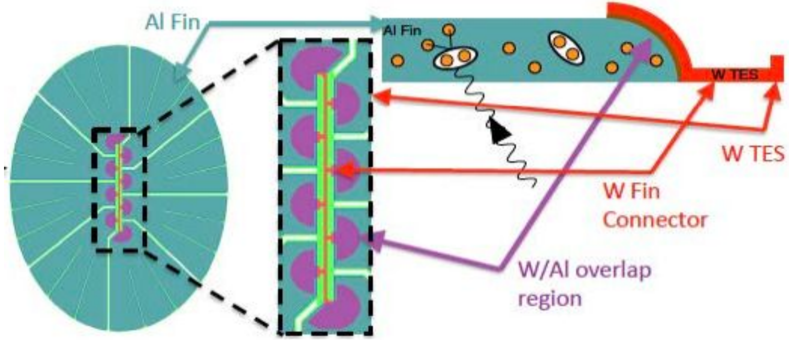

35% Al fin coverage (compared to 4% in iZIP)

Decreases phonon collection time

Better position information

Tighter energy resolution

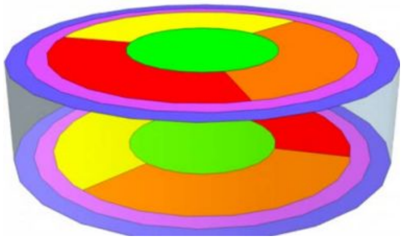

2-sided bias giving uniform E-Field

Phonon readout: high-voltage cryogenic semiconductor

Representative experiments: SuperCDMS HV,

Signal Anatomy

E_R → e-h pairs + prompt phonons → e-h drift in HV →additional NTL phonon → QET/TES phonon readout → E_{phonon}

Response from particle interaction

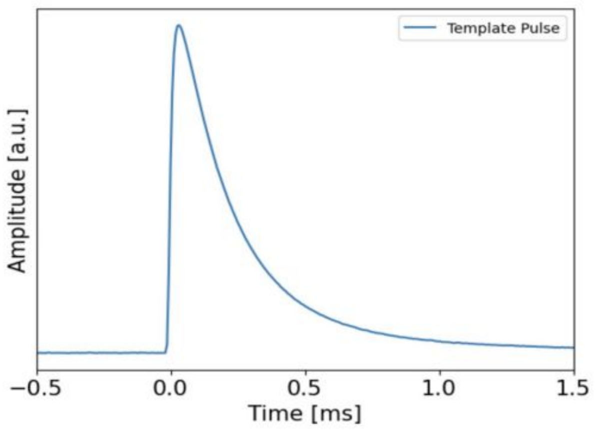

SQUIDS: Height of pulse gives estimate of energy

Example Energy Spectrum

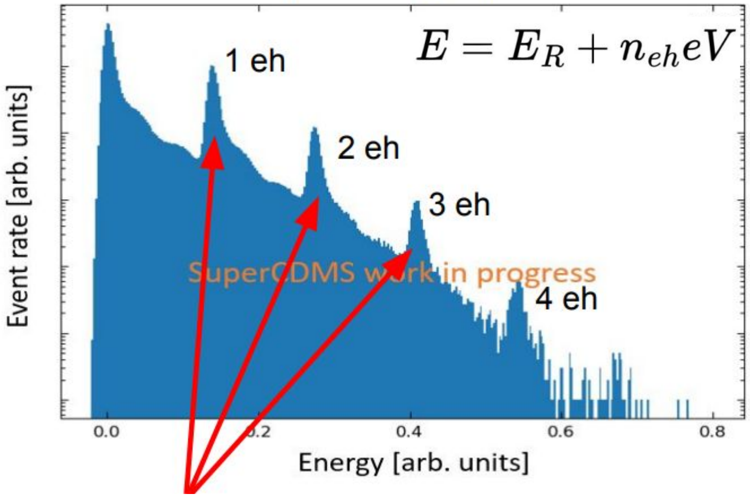

Peaks correspond to number of electron-hole (eh) pairs produced

Phonon + Channel readout: SuperCDMS Expermient

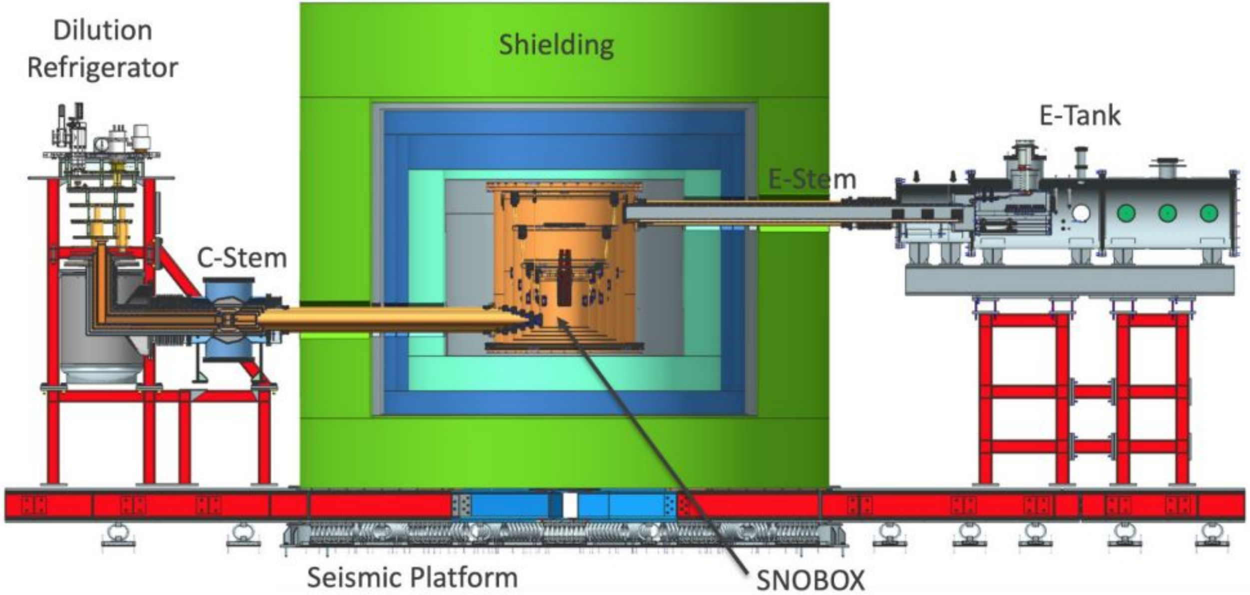

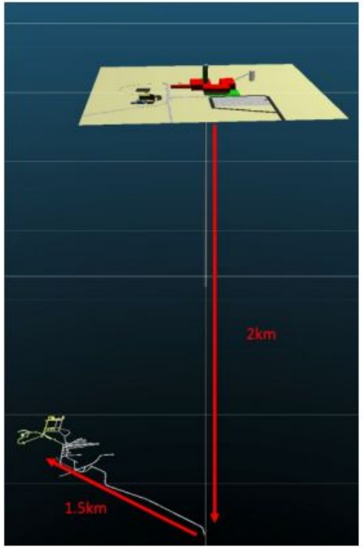

2 km of rock overburden (6000 m.w.e) at SNOLAB, Canada
→ Factor of 100 reduction in muon flux compared to previous generation

Phonon + Channel readout: SuperCDMS Experiment

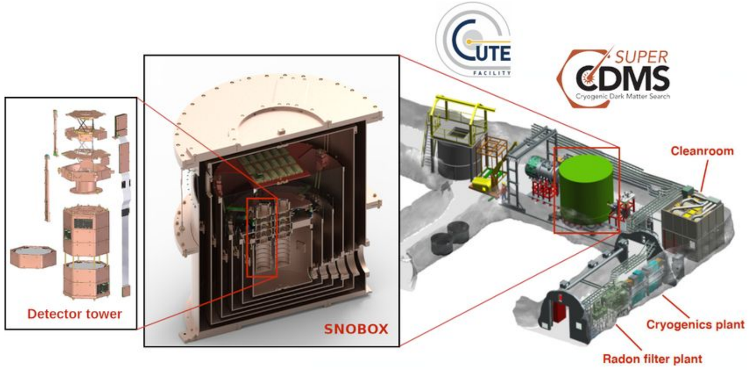

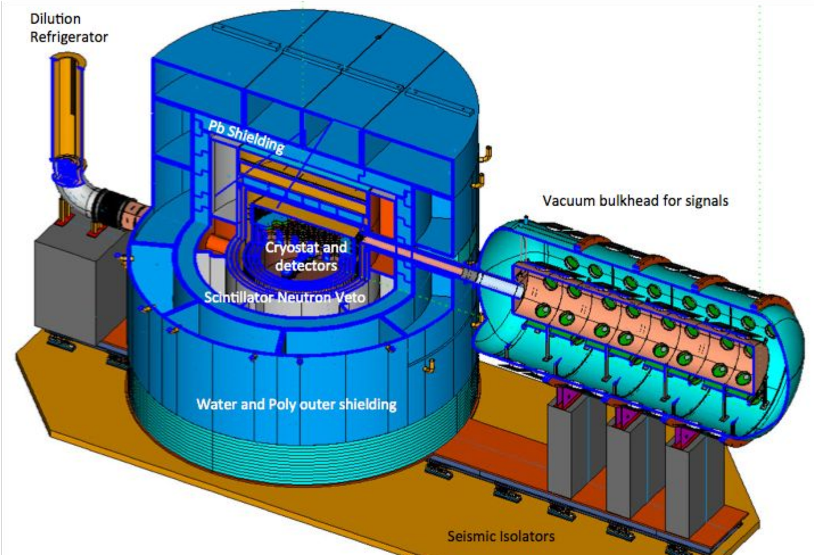

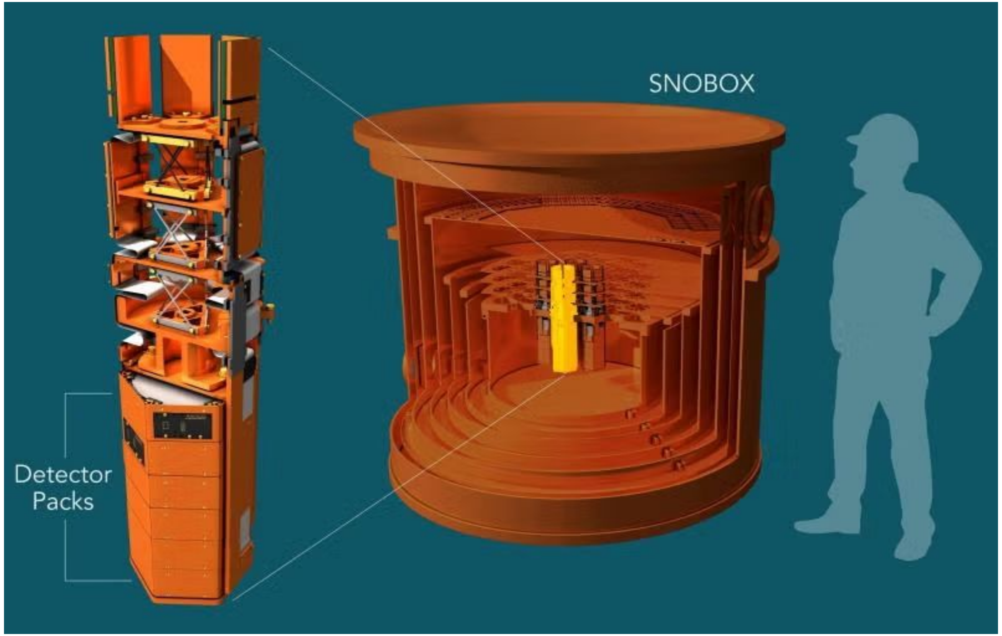

Phonon + Channel readout: SuperCDMS Experiment

- **4 towers, 6 detectors each**
  - 10 Ge iZIPs
  - 2 Si iZIPs
  - 8 Ge HVs
  - 4 Si HVs
- **28.8 kg payload**
  - 0.6 kg per Si detector
  - 1.4 kg per Ge detector
- **Channel segmentation for position reconstruction**
  - 12 phonon channels
  - 4 charge channels on iZIPs

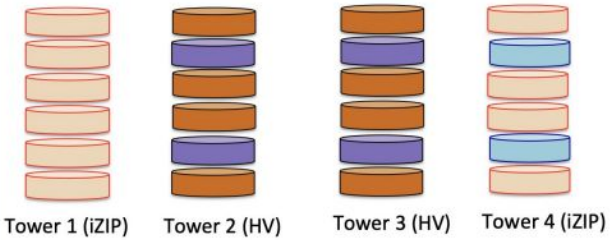

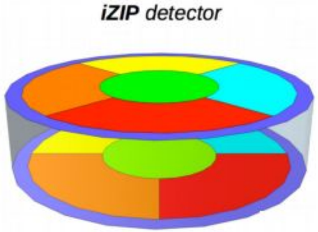

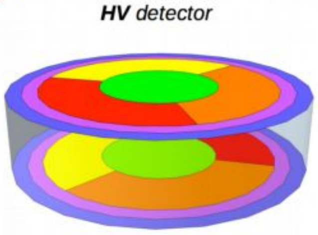

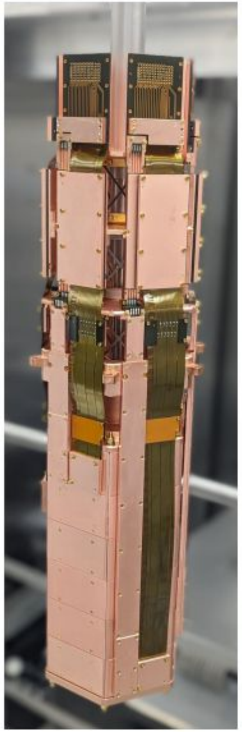

Were detector technologies compete in WIMP searches

Detector performance is not one-dimensional

High-mass WIMPs: sensitivity is mainly exposure- and background-limited
→ large, ultra-clean LXe/LAr targets dominate.

Low-mass WIMPs: sensitivity is mainly threshold- and quenching-limited
→ cryogenic semiconductors, CCDs, and low-threshold detectors become competitive.

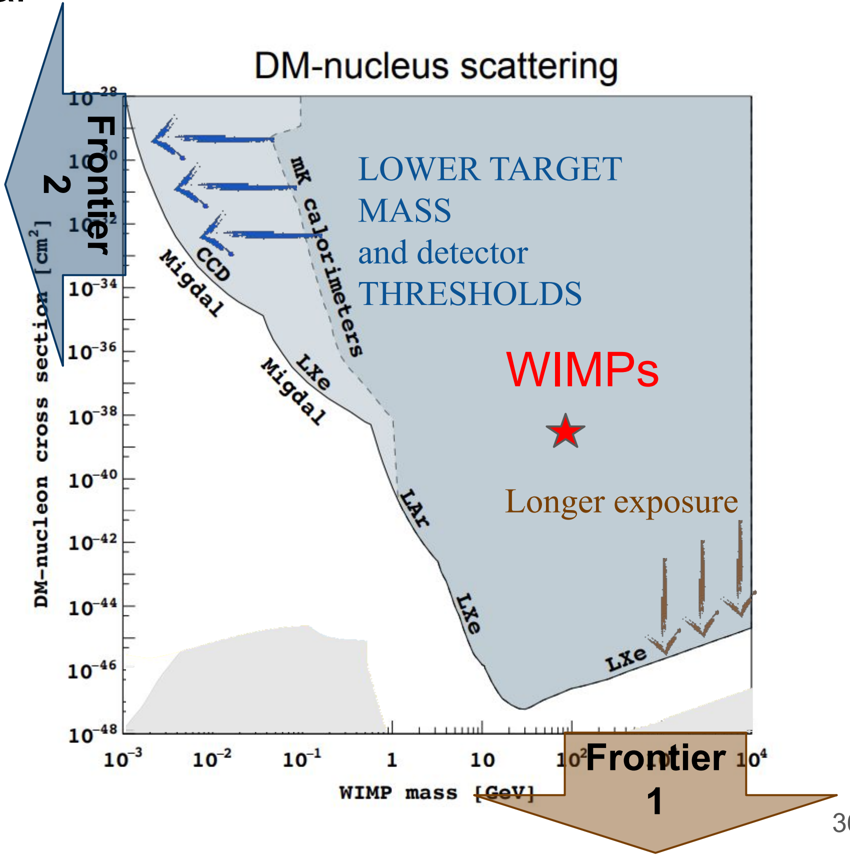

Different technologies push different frontiers: mass, threshold, background rejection, and stability.

Frontier 1: LEE Frontier for current WIMP searches

Low Energy Excess mitigation is key to opening up the sub-GeV regime for discovery

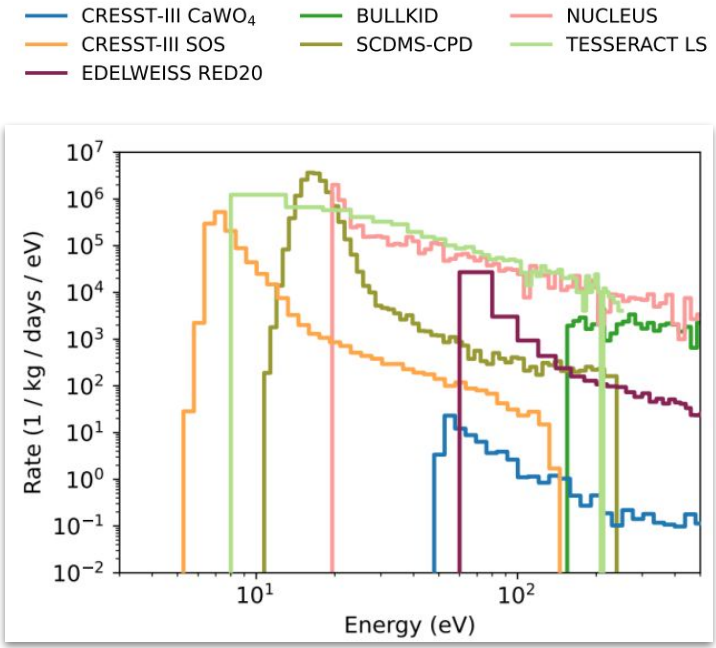

Impact on the DM sensitivity: in the LEE presence the DM sensitivity is worsened by orders of magnitude!

And exposure increase does not help in the sub-GeV DM regime

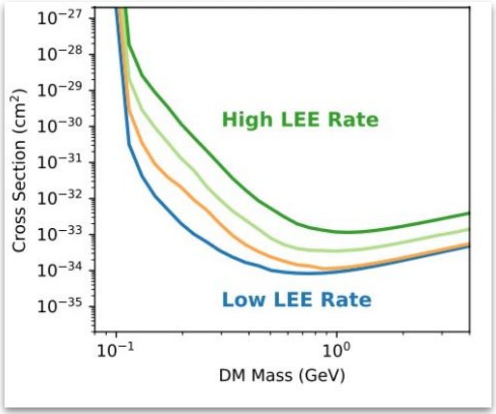

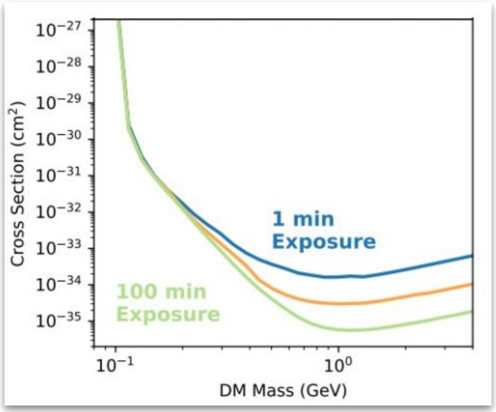

Frontier 2: Beyond nuclear recoils
Electron recoils and quantum excitations

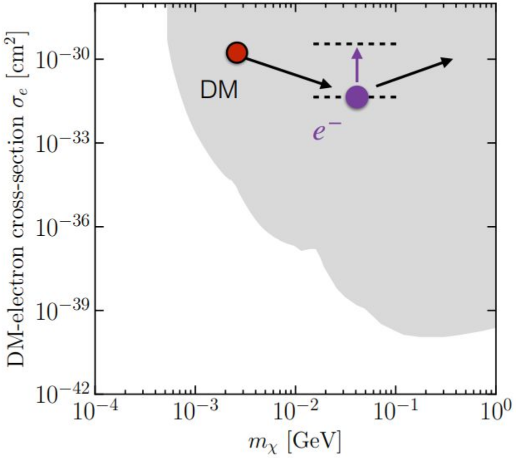

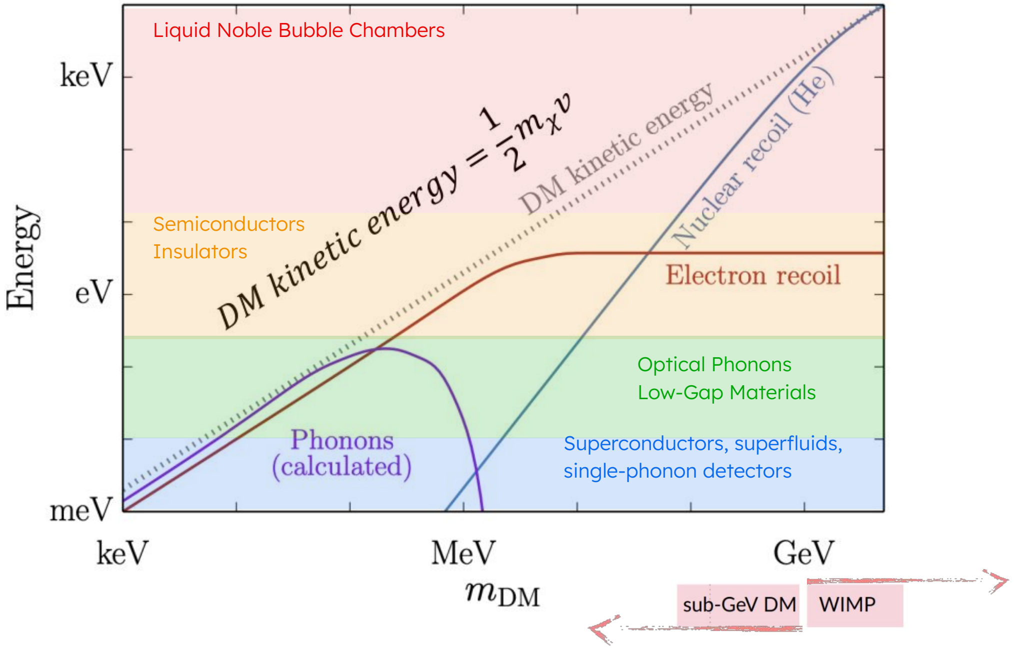

Adapted from: arXiv:1904.07915

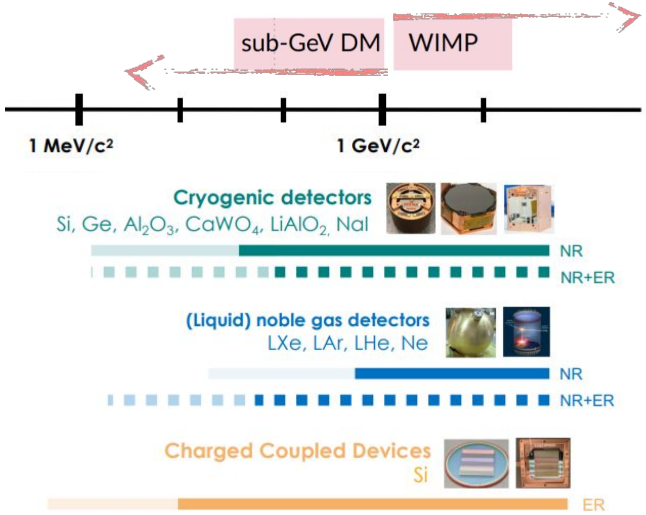

Summary: detector technology defines the physics reach

- A WIMP signal is not measured directly: it is converted into charge, light, phonons, heat, or topology.
- ER and NR depositions produce different visible signals because of quenching and channel-dependent yields.
- CCDs, scintillators, noble-liquid TPCs, and cryogenic semiconductors optimize different trade-offs.
- Large exposures dominate high-mass WIMP searches; low thresholds dominate the low-mass regime.
- Future progress requires controlling the low-energy excess and developing sensors for new quantum excitations.